Polynuclear Organometallic Helices by Means of Novel Coupling Reactions of Cyclomanganated Complexes with Aryl-Substituted Diazoalkanes: Syntheses of New Manganospiralenes and Appended (η^5-fluoren-9-yl)M(CO)$_3$ Complexes (M = Mn, Re)

Christophe Michon,[†] Jean-Pierre Djukic,*[,†] Zoran Ratkovic,[†,‡] Jean-Paul Collin,[§] Michel Pfeffer,*[,†] André de Cian,[||] and Jean Fischer[||,⊥]

UMR 7513 CNRS, Institut de Chimie de Strasbourg, Université Louis Pasteur 4, rue Blaise Pascal, F-67070 Strasbourg Cedex, France

Dirk Heiser,[#] Karl Heinz Dötz,*[,#] and Martin Nieger[#,¶]

Kekulé Institut für Organische Chemie und Biochemie und Institut für Anorganische Chemie der Universität Bonn, Gerhard-Domagk Strasse 1, D-53121 Bonn, Germany

Received February 13, 2002

Novel reactions of various *cis*-(LC)Mn(CO)$_4$ complexes (LC = a three-electron chelating ligand) with diazodiphenylmethane and 9-diazofluorene allowed the synthesis of a new type of oligomeric polynuclear manganospiralene derived from quinoxaline and the ready preparation of a new class of appended (η^5-fluorenyl)Mn(CO)$_3$ complexes. Hence, bis-cyclomanganated 2,3-diphenylquinoxaline cleanly reacted to afford a dinuclear dispiralene in which the heterocycle is embedded between two phenyl rings introduced by diphenyldiazomethane. The reaction of cyclomanganated and rhenated aromatic compounds with 9-diazofluorene is shown to proceed efficiently under thermolytic conditions, which promote the departure of one molecule of CO and the subsequent coordination of a fluorenylidene fragment. Further rearrangements consisting of a cis-migration step and of a series of haptotropic shifts lead to the final appended (η^5-fluorenyl)M(CO)$_3$ complex (M = Mn, Re). This new C−C bond-forming reaction has enabled the synthesis of a pentacyclic helical compound derived from bis-cyclomanganated 2,3-diphenylquinoxaline and whose conformation could be locked by coordination to Ag$^+$, affording a hybrid inorganic−organometallic polyhelix. An overview of the electrochemical properties of selected mono- and binuclear spiralenes is disclosed and shows that most spiralenes display electrochemically reversible reduction processes. An ESR analysis of the radical anion of a dinuclear spiralene indicated that the reduction process is ligand-centered and the spin density essentially located at the heterocycle. The structures of new spiralenes and appended (fluorenyl)M(CO)$_3$complexes, obtained by crystal X-ray diffraction techniques, are described.

Introduction

Assembled arrays of aromatics obtained by means of metal coordination at the nanoscale or by large-scale polymerization are of interest for the design of electroactive materials for optoelectronics.[1] As shown by the early reports of Heeger and other researchers, n- or p-doped layers of organic polymers can be readily obtained by either electrochemical or chemical reduction or oxidation of organic polymeric substrates. Electroluminescence is another interesting property, which finds its applications in electronic display devices. Polymers containing polyaza aromatic units are particularly suitable for applications in so-called PLEDs as precursors for n-doped conducting media and electroluminescent layers.

Our long interest for the chemistry of transition-metal centers chelated by aza-heterocyclic aromatic ligands[2] naturally leads us to consider bringing a contribution to this swiftly expanding field by applying some of our recent achievements in the chemistry of Mn(I) chelates.[3] The keystone of our project is the chemistry of a new family of helical organometallic molecules, the metallospiralenes, whose intramolecular ring $\pi-\pi$ stacking feature may establish the base for the design of a new class of electron conducting medium.[4] We recently

* To whom correspondence should be addressed. E-mail: J.-P.D., djukic@chimie.u-strasbg.fr; M.P., pfeffer@chimie.u-strasbg.fr; K.H.D., doetz@uni-bonn.de.
[†] Laboratoire de Synthèses Métallo-induites.
[‡] Permanent address: Faculty of Science of the University of Kragujevac, R. Domanovica 12, YU-34000 Kragujevac, FR Yugoslavia.
[§] Laboratoire de Chimie Organo-Minérale.
[||] Laboratoire de Cristallochimie.
[⊥] To whom requests pertaining to X-ray diffraction analyses should be sent. E-mail: for compounds **1b**,**c**, **2b**, and **3c**−**e**, J.F. at fischer@chimie.u-strasbg.fr; for compounds **5a**,**c**, M.N. at m.nieger@uni-bonn.de.
[#] Kekulé Institut für Organische Chemie und Biochemie.
[¶] Institut für Anorganische Chemie.

10.1021/om020116z CCC: $22.00
Publication on Web 07/23/2002

reported on the mechanistic issues of the formation of manganospiralenes, a class of organometallic helical molecules consisting of a polyaromatic ligand tightly coiled around a $M(CO)_3$ scaffold.[5]

These helical molecules arise from the stereoselective insertion of an alkylidene species into the C_{Ar}−Mn bond of a cyclomanganated *cis*-(LC)$Mn(CO)_4$ complex, in which LC stands for a three-electron chelating ligand (Scheme 1). The alkylidene transient species can be formed by two different experimental approaches: (1) the classical "E. O. Fischer method", which consists of the sequential treatment of the starting metal−carbonyl complex with an organolithium nucleophile, followed by treatment with a hard alkylation agent, and (2) the thermolysis of the *cis*-(LC)$Mn(CO)_4$ complex in the presence of a diazoalkane. We successfully applied the first method in many cases with various types of organolithium reagents.[6] We found, however, the second method to be softer and more reliable, as we now aim in the first stage to build elaborated oligomeric spiralenes and in the second stage to prepare the parent organometallic polymers.[4] Such a method involves neutral diazoalkanes that have proven their versatility in numerous applications in organic synthesis as precursors of reactive triplet alkylidene[7] and, of course, in organometallic chemistry.[8] In the present article we report on novel reactions of various Mn(I) chelates with diphenyldiazomethane[9] and 9-diazofluorene,[10] which allowed the ready preparation of a new class of appended (η^5-fluorenyl)$Mn(CO)_3$ complexes, and on the synthesis of a new type of oligomeric polynuclear spiralene[3c] derived from quinoxaline. We disclose an overview of the electrochemical properties of selected mono- and binuclear spiralenes, and we further present the first synthesis of a hybrid inorganic−organometallic polyhelix consisting of a single-strand arrangement of pentacyclic helices locked by metal coordination.

Scheme 1

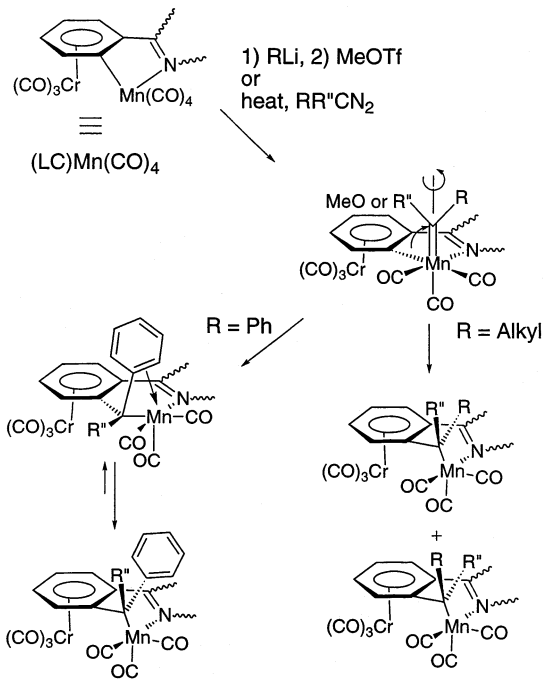

Results and Discussion

Reaction of Ph_2CN_2 with Cyclomanganated Phenylpyridines. The use of diazoalkanes[11] for the synthesis of transition-metal alkylidene complexes was described by Herrmann and co-workers in the 1970s.[12] The method consists of a reaction between a transition-metal complex possessing at least one available coordination site and an alkylidene precursor such as a diazoalkane. In reports dealing with $M(CO)_nL_m$-type

(1) (a) Shirakawa, H.; Louis, E. J.; MacDiarmid, A. G.; Chiang, C. K.; Heeger, A. G. *Chem. Commun.* **1977**, 578. (b) Chiang, C. K.; Fincher, C. R.; Park, Y. W.; Heeger, A. J.; Shirakawa, H. Louis, E. J. *Phys. Rev. Lett.* **1977**, *39*, 1098. (c) Petit, M. A.; Clarisse, C.; Templier, F. *J. Electrochem. Soc.* **1993**, *140*, 2498. (d) Kanbara, T.; Inoue, T.; Sugiyama, K.; Yamamoto, T. *Synth. Met.* **1995**, *71*, 2207. (e) Murata, H.; Ukishima, S.; Hirano, H.; Yamanaka, T. *Polym. Adv. Technol.* **1997**, *8*, 459. (f) Yamamoto, T.; Sugiyama, K.; Kushida, T.; Inoue, T.; Kanbara, T. *J. Am. Chem. Soc.* **1996**, *118*, 3930. (g) Yamamoto, T.; Zhou, Z. H.; Kanbara, T.; Shimura, M.; Kizu, K.; Maruyama, T.; Nakamura, Y.; Fukuda, T.; Lee, B. L.; Ooba, N.; Tomaru, S.; Kurihara, T.; Kaino, T.; Kubota, K.; Sasaki, S. *J. Am. Chem. Soc.* **1996**, *118*, 10389. (h) Wu, A.; Akagi, T.; Jikei, M.; Kakimoto, M. A.; Imai, Y.; Ukishima, S.; Takahashi, Y. *Thin Solid Films* **1996**, *273*, 214. (i) Kraft, A.; Grimsdale, A. C.; Holmes, A. B. *Angew. Chem.* **1998**, *110*, 416; *Angew. Chem., Int. Ed.* **1998**, *37*, 402. (j) van Mullekom, H. A. M.; Vekemans, J. A. J. M.; Meijer, E. W. *Chem. Eur. J.* **1998**, *4*, 1235. (k) Greiner, A. *Polym. Adv. Technol.* **1998**, *9*, 371. (l) Thelakkat, M.; Schmidt, H.-W. *Polym. Adv. Technol.* **1998**, *9*, 429. (m) Lee, B. L.; Yamamoto, T. *Macromolecules* **1999**, *32*, 1375. (n) Zhang, C. Y.; Tour, J. M. *J. Am. Chem. Soc.* **1999**, *121*, 8783. (o) Leung, L. M.; Kwong, C. F.; Kwok, C. C.; So, S. K. *Displays* **2000**, *21*, 199. (p) Guo, T.-F.; Chang, S. C.; Yang, Y.; Kwong, R. C.; Thompson, M. E. *Org. Electron.* **2000**, *1*, 15. (q) Bernius, M. T.; Inbasekaran, M.; O'Brien, J.; Wu, W. *Adv. Mater.* **2000**, *12*, 1737. (r) Le Barny, P.; Dentan, V.; Facoetti, V.; Vergnolle, M.; Veriot, G.; Servet, B.; Pribat, D. *C.R. Acad. Sci. Paris, t. 1, Ser. IV* **2000**, 493. (s) Heeger, A. J. *Angew. Chem., Int. Ed.* **2001**, *40*, 2591. (t) Ng, P. K.; Gong, X.; Chan, S. H.; Szeman Lam, L.; Chan, W. K. *Chem. Eur. J.* **2001**, *7*, 4358.

(2) (a) Pfeffer, M. *Recl. Trav. Chim. Pays-Bas* **1990**, *109*, 567. (b) Pfeffer, M. *Pure Appl. Chem.* **1992**, *94*, 335. (c) Spencer, J.; Pfeffer, M. *Adv. Met.-Org. Chem.* **1998**, *6*, 103. (d) Dupont, J.; Pfeffer, M.; Spencer, J. *Eur. J. Inorg. Chem.* **2001**, 1917.

(3) (a) Djukic, J. P.; Maisse, A.; Pfeffer, M.; De Cian, A.; Fischer, J. *Organometallics* **1997**, *16*, 657. (b) Djukic, J. P.; Maisse, A.; Pfeffer, M. *J. Organomet. Chem.* **1998**, *567*, 65. (c) De Cian, A.; Djukic, J.-P.; Fischer, J.; Pfeffer, M.; Dötz, K. H. *Chem. Commun.* **2002**, 638.

(4) Djukic, J. P.; Michon, C.; Maisse-François, A.; Allagapen, R.; Pfeffer, M.; Dötz, K. H.; De Cian, A.; Fischer, J. *Chem. Eur. J.* **2000**, *6*, 1064.

(5) Djukic, J. P.; Maisse-François, A.; Pfeffer, M.; Dötz, K. H.; De Cian, A.; Fischer, J. *Organometallics* **2000**, *19*, 5484.

(6) (a) Djukic, J. P.; Dötz, K. H.; Pfeffer, M.; De Cian, A.; Fischer, J. *Organometallics* **1997**, *16*, 5171. (b) Djukic, J. P.; Dötz, K. H.; Pfeffer, M.; De Cian, A.; Fischer, J. *Inorg. Chem.* **1998**, *37*, 3649. (c) Djukic, J. P.; Maisse, A.; Pfeffer, M.; Dötz, K. H.; Nieger, M. *Organometallics* **1999**, *18*, 2786. (d) Djukic, J. P.; Maisse, A.; Pfeffer, M.; Dötz, K. H.; Nieger, M. *Eur. J. Inorg. Chem.* **1998**, 1781.

(7) (a) Regitz, M.; Maas, G. In *Diazo Compounds, Properties and Synthesis*; Academic Press: Orlando, FL, 1986. (b) *The Chemistry of Diazonium and Diazo Groups, Part 1*; Patai, S., Ed.; Wiley: Chichester, U.K., 1978. (c) Closs, G. L.; Coyle, J. J. *J. Am. Chem. Soc.* **1966**, *31*, 1966. (d) Fiedler, B.; Wei*β*, D.; Beckert, R. *Liebigs Ann./Recl.* **1997**, 613. (e) Thoraval, J. Y.; Nagai, W.; Yeung Lam Ko, Y. Y. C.; Carrié, R. *Tetrahedron* **1990**, *46*, 3859. (f) Froussios, C.; Kolovos, M. *Tetrahedron Lett.* **1989**, *30*, 3413. (g) De Jongh, D. C.; Van Fossen, R. Y. *Tetrahedron* **1972**, *28*, 3603. (h) Cava, M. P.; Litle, R. L.; Napier, D. R. *J. Am. Chem. Soc.* **1958**, *80*, 2257. (i) Ishiguro, K.; Ikeda, M.; Sawaki, Y. *J. Org. Chem.* **1992**, *57*, 3057. (j) Hirai, K.; Tomioka, H.; Ohashi, Y. *J. Am. Chem. Soc.* **2001**, *123*, 6904. (k) Nishino, S. I.; Moritani, I.; Nishino, M. *Tetrahedron* **1971**, *27*, 5131. (l) Regitz, M.; Liedhegener, A. *Tetrahedron* **1967**, *23*, 2701. (m) Moritani, I.; Murahashi, S. I.; Yoshinaga, K.; Ashitaka, H. *Bull. Chem. Soc. Jpn.* **1967**, *40*, 1506. (n) Plater, M. J.; Kemp, S.; Lattmann, E. *J. Chem. Soc., Perkin Trans. 1* **2000**, 971. (o) Itakura, H.; Mizuno, H.; Hirai, K.; Tomioka, H. *J. Org. Chem.* **2000**, *65*, 8797.

(8) (a) Sutton, D. *Chem. Rev.* **1993**, *93*, 995. (b) Mizobe, Y.; Ishii, Y.; Hidai, M. *Coord. Chem. Rev.* **1995**, *139*, 281. (c) Dartiguenave, M.; Menu, M. J.; Deydier, E.; Dartiguenave, Y.; Siebald, H. *Coord. Chem. Rev.* **1998**, *178−180*, 623.

(9) Miller, J. B. *J. Org. Chem.* **1959**, *24*, 560.

(10) Staudinger, H.; Kupfer, O. *Ber. Dtsch. Chem. Ges.* **1911**, *44*, 2197.

(11) Putala, M.; Lemenovskii, D. A. *Russ. Chem. Rev. (Engl. Transl.)* **1994**, *63*, 197.

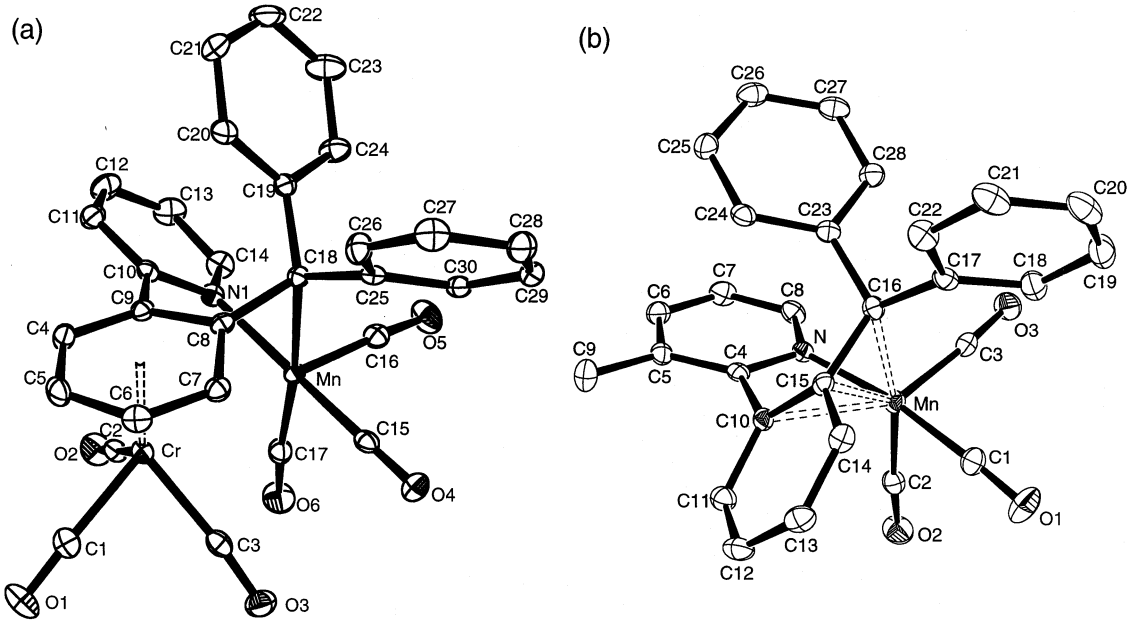

Figure 1. (a) ORTEP diagram of complex **1b** displayed at the 30% probability level with the corresponding atom numbering. Hydrogen atoms have been omitted for clarity purposes. Selected interatomic distances (Å): Mn−Cr, 3.047(3); Mn−C18, 2.182(2); Mn−C8, 2.356(2); Mn−N, 2.074(1); Cr−C8, 2.443(2); C8−C18, 1.452(3); C19−C10, 2.896 (3); Mn−C9, 2.904 (3); Cr−C_{Ar} (average), 2.226. Selected interatomic angles (deg): C2−Cr−C3, 93.93(8); C1−Cr−C2, 84.52(9); C1−Cr−C3, 81.46-(9); C7−C8−C9, 113.9(2). Selected torsion angles (deg): C10−C9−C8−C18, 19.6; C8−C9−C10−N, 38.0. Angles between mean planes P_1 (C10−C11−C12−C13−C14−N), P_2 (C9−C8−C7−C6−C5−C4) and P_3 (C19−C20−C21−C22−C23−C24) (deg): P_1-P_2, 37.6; P_1-P_3, 37.0. (b) ORTEP diagram of complex **2b** displayed at the 30% probability level with the corresponding atom numbering. Hydrogen atoms have been omitted for clarity purposes. Selected interatomic distances (Å): Mn−C16, 2.173(2); Mn−C15, 2.221(2); Mn−C10, 2.361(2); Mn−N, 2.019(2); C15−C16, 1.468(3); C4−C23, 2.996(3). Selected interatomic angles (deg): C14−C15−C10, 114.9(2); N−Mn−C16, 85.67(8). Selected torsion angles (deg): C16−C15−C10−C4, 12.6; C15−C10−C4−N, 55.2.

complexes, the necessary vacant site at the metal center is created by the photolytic decoordination of one molecule of CO.[13] The formation of transient metal−alkylidene species by direct reaction of diazoalkanes with electron-deficient metal centers constitutes the essence of "metal-carbenoid" based transformations in organic synthesis.[14] Cyclomanganated complexes of the formula *cis*-(LC)$Mn(CO)_4$ can undergo a mono-decoordination of CO under chemical,[15] photolytic[16] or thermolytic[17] conditions enabling thus various sorts of exogenous ligands to interact with the Mn(I) center. We previously found that the thermolytic method was indeed well suited for a reaction between cyclomanganated 2-[tricarbonyl(η^6-phenyl)chromium]pyridine (**1a**) and diazodiphenylmethane (eq 1).[4]

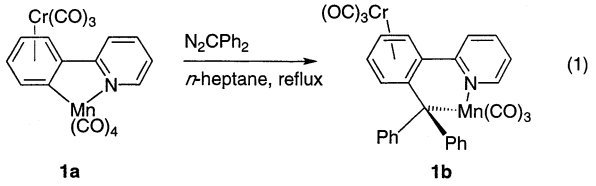

(1)

The product, e.g. **1b**, which was fully characterized spectroscopically and analytically, displayed physical properties similar to those of all known heterobimetallic spiralenes.[4] We succeeded in resolving the structure of this complex by X-ray diffraction methods. An ORTEP diagram is shown in Figure 1a. Acquisition and processing data are listed in Table 1. The overall shape of this heterobimetallic species is helical. The two metals face each other: the Cr atom occupies one of the equatorial positions of the pseudo-octahedron centered at the Mn atom. The Cr−Mn distance of 3.047(2) Å is character-

(12) (a) Herrmann, W. A. *Angew. Chem.* **1974**, *86*, 556; *Angew. Chem., Int. Ed. Engl.* **1974**, *13*, 599. (b) Herrmann, W. A. *Angew. Chem.* **1978**, *90*, 855; *Angew. Chem., Int. Ed. Engl.* **1978**, *17*, 800. (c) Herrmann, W. A. *Chem. Ber.* **1975**, *108*, 486. (d) Herrmann, W. A.; Weidenhammer, K.; Ziegler, M. L. *Z. Anorg. Allg. Chem.* **1980**, *460*, 200. (e) Herrmann, W. A. *Chem. Ber.* **1975**, *108*, 3412. (f) Herrmann, W. A. *Pure Appl. Chem.* **1982**, *54*, 65. (g) Herrmann, W. A.; Planck, J.; Kriechbaum, G. W.; Ziegler, M. L.; Pfisterer, H.; Atwood, J. L.; Rogers, R. D. *J. Organomet. Chem.* **1984**, *264*, 327.

(13) (a) Wrighton, M. *Chem. Rev.* **1974**, *74*, 401. (b) Strohmeier, W.; von Hobe, D.; Schönauer, G.; Laporte, H. *Z. Naturforsch.* **1962**, *17b*, 502. (c) Strohmeier, W.; Guttenberger, J. F. *Chem. Ber.* **1964**, *97*, 1256. (d) Strohmeier, W.; Guttenberger, J. F. *Chem. Ber.* **1964**, *97*, 1871. (e) Strohmeier, W.; Gerlach, K. *Chem. Ber.* **1961**, *94*, 398. (f) Strohmeier, W.; von Hobe, D. *Chem. Ber.* **1961**, *94*, 2031. (g) Giordano, P. J.; Wrighton, M. S. *Inorg. Chem.* **1977**, *16*, 160. (h) Bengali, A. A. *Organometallics* **2000**, *19*, 4000. (i) Braunschweig, H.; Ganter, B. *J. Organomet. Chem.* **1997**, *545*, 163. (j) Hofmann, P. *Angew. Chem.* **1977**, *89*, 551; *Angew. Chem., Int. Ed. Engl.* **1977**, *16*, 536. (k) Ward, T. R.; Schafer, O.; Daul, C.; Hofmann, P. *Organometallics* **1997**, *16*, 3207. (l) Young, K. M.; Wrighton, M. S. *Organometallics* **1989**, *8*, 1063. (m) Yang, H.; Asplund, M. C.; Kotz, K. T.; Wilkens, M. J.; Frei, H.; Harris, C. B. *J. Am. Chem. Soc.* **1998**, *120*, 10154. (n) Fischer, E. O.; Herberhold, M. In *Essays in Coordination Chemistry*, Exp. Suppl. IX: Birkenheuser-Verlag: Basel, Switzerland, 1964.

(14) (a) Doyle, M. P. *Chem. Rev.* **1986**, *86*, 919. (b) Doyle, M. P. *Recl. Trav. Chim. Pays-Bas* **1991**, *110*, 305. (c) Tomilov, Yu. V.; Dokichev, V. A.; Dzemilev, U. M.; Nefedov, O. M. *Russ. Chem. Rev. (Engl. Transl.)* **1993**, *62*, 799. (d) Doyle, M. P. In *Catalytic Asymmetric Synthesis*; Ojima, I., Ed.; VCH: New York, 1993; pp 63−99. (e) Ye, T.; McKervey, M. A. *Chem. Rev.* **1994**, *94*, 1091. (f) Bernardi, F.; Bottoni, A.; Miscione, G. P. *Organometallics* **2000**, *19*, 5529.

(15) (a) Liebeskind, L. S.; Gadaska, J. R.; McCallum, J. S. *J. Org. Chem.* **1989**, *54*, 669. (b) Cambie, R. C.; Metzler, M. R.; Tutledge, P. S.; Woodgate, P. D. *J. Organomet. Chem.* **1990**, *381*, C28.

(16) Grigsby, W. J.; Main, L.; Nicholson, B. K. *Organometallics* **1993**, *12*, 397.

(17) Cambie, R. S.; Metzler, M. R.; Rutledge, P. S.; Woodgate, P. D. *J. Organomet. Chem.* **1992**, *429*, 41.

Table 1. Acquisition and Refinement Data for the X-ray Diffraction Analyses of Complexes 1b,c, 2b, 3c−e, and 5a,c[a]

	1b	1c	2b	3c	3d	3e	5a	5c
formula	$C_{30}H_{18}CrMnNO_6$	$C_{30}H_{16}CrMnNO_6$	$C_{28}H_{20}MnNO_3$	$C_{52}H_{32}Mn_2N_2O_6$	$C_{52}H_{28}Mn_2N_2O_6 \cdot CH_2Cl_2$	$C_{53}H_{31}AgMn_2N_2O_6 \cdot BF_4 \cdot 2CH_3OH$	$C_{19}H_{10}CrNO_7Re$	$C_{32}H_{18}CrNO_7Re$
mol wt	595.42	593.40	473.41	890.72	971.62	1176.48	602.48	766.67
cryst syst	monoclinic	monoclinic	orthorhombic	monoclinic	orthorhombic	orthorhombic	monoclinic	triclinic
space group	$P2_1/c$	$P2_1/c$	$Pbca$	$P2_1/n$	$Pbca$	$P2_12_12_1$	$P2_1/c$	$P\bar{1}$
a (Å)	8.9761(2)	9.6538(3)	11.8883(2)	15.6887(7)	14.8379(2)	13.6186(5)	14.5814(5)	10.6761(1)
b (Å)	14.3301(5)	15.0319(5)	17.0308(2)	16.7698(9)	35.4532(3)	15.1375(7)	7.1064(1)	15.5375(2)
c (Å)	19.8900(7)	17.5379(5)	21.9813(4)	15.9857(7)	16.3323(5)	25.032(1)	18.5035(6)	16.4606(2)
α (deg)								76.462(1)
β (deg)	100.134(6)	100.773(5)		93.588(5)			106.175(1)	85.527(1)
γ (deg)								84.046(1)
V (Å^3)	2518.5(3)	2500.2(1)	4450.5(1)	4197.5(3)	8591.6(3)	5160.5(4)	1841.46(9)	2636.22(5)
Z	4	4	8	4	8	4	4	4
color	red	orange	red	dark blue	yellow	red	orange	orange
cryst dimens (mm)	0.20 × 0.09 × 0.05	0.18 × 0.12 × 0.08	0.20 × 0.20 × 0.16	0.20 × 0.14 × 0.10	0.16 × 0.13 × 0.10	0.12 × 0.10 × 0.08	0.25 × 0.15 × 0.10	0.20 × 0.10 × 0.04
D_{calcd} (g cm^{-3})	1.57	1.58	1.41	1.41	1.50	1.51	2.173	1.932
F_{000}	1208	1200	1952	1824	3952	2372	1144	1488
μ (mm^{-1})	0.980	0.987	0.624	0.657	0.769	0.930	7.201	5.054
temp. (K)	173	173	173	294	173	173	123	123
scan mode				ψ scans				
hkl limits	−11 to +11/ −17 to +18/ −25 to +25	−12 to +12/ −17 to +19/ −22 to +22	−16 to +16/ −22 to +22/ −30 to +30	−20 to +20/ −21 to +20/ −20 to +20	−19 to +19/ −21 to +21/ −45 to +45	−17 to +17/ −19 to +19/ −32 to +32	−17 to +17/ −8 to +7/ −22 to +22	−12 to +12/ −18 to +18/ −19 to +19
θ limits (deg)	2.5−27.46	2.5−27.46	2.5−30.03	2.5−27.51	2.5−27.48	2.5−27.48	2.91−25.00	2.55−25.00
no. of data measd	10 143	10 230	12 128	16 708	19 157	11 811	15 396	57 909
no. of unique data	4184	3727	3412	3947	3614	3656	3245	9270
no. of variables	352	352	298	559	586	634	263	759
R	0.028	0.033	0.036	0.035	0.051	0.058	0.0210	0.0266
R_w	0.040	0.060	0.050	0.040	0.082	0.080	0.0563	0.0711
GOF	1.011	1.073	1.057	1.040	1.415	1.513	1.110	1.037
largest peak in final diff map (e Å^{-3})	0.562	0.357	0.404	0.289	0.589	0.959	1.762	1.225

[a] All measurements were performed with a Nonius KappaCCD diffractometer using Mo Kα graphite-monochromated radiation (λ = 0.710 73 Å).

istic of a weak intermetal interaction and remains in the range of previously reported data.[6] An interplanar angle of 37° and the C10−C19 distance of 2.896(3) Å characterize the overlap of one phenyl ring and the pyridyl ring. The shortest distances between the last two mean planes are indeed lower than the optimal distance of 3.6 ± 0.1 Å observed in most cases for parallel face-to-face $\pi-\pi$ stacking interactions.[18]

The mononuclear complex **2a** displayed a similar behavior when treated with Ph_2CN_2 in refluxing *n*-heptane (eq 2). The orange-yellow product of the reaction was readily identified as the mononuclear spiralene **2b** (Figure 1b). A combination of IR, ^{1}H and ^{13}C NMR, and X-ray diffraction analyses assessed that in solution as well as in the solid state the Mn(I) center is bonded to the benzylic position (atom C16 in Figure 1b) and the two vicinal aromatic carbons (atoms C15 and C10) of the phenylpyridine fragment. The temperature dependence of the shape and multiplicities of ^{1}H NMR signals of **2b** produced by the overlap of one phenyl group with the heterocycle is an additional indication of the helical shape of the molecule. In the structure depicted in Figure 1b, the inter-ring distance C4−C23 has a value of 2.996 Å. A solution IR spectrum of **2b**, carried out in CH_2Cl_2, further ascertains that the Mn(I) center is bonded to the two above-mentioned aromatic carbon atoms of the phenylpyridine ring: the CO stretching band at 2000 cm^{-1} is typical of mononuclear Mn(I) spiralenes.

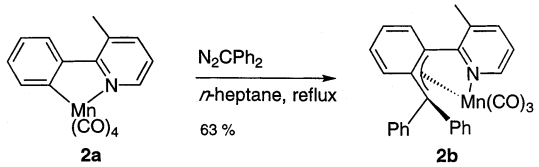

(2)

Reaction of Ph_2CN_2 with Pro-Helical Bis-Cyclomanganated 2,3-Diphenylquinoxaline. Birth of a Homometallic Bis-Manganospiralene. It is well established that the conformational stability of helicenes depends on the number of fused rings.[19] It is also directly related to geometrical parameters such as the pitch, the number of turns, and the radius of the helix, which defines with the handedness the "chirality" of helicenes.[20] Among all helicenes, pentahelicenes possess the lowest barriers to conformational change and a dynamic behavior in solution. Bis-cyclometalated 2,3-diphenylquinoxaline and -pyrazine complexes can be considered as dimetalla analogues of pentahelicenes. Cyclopalladated 2,3-diphenylpyrazine, for example, has been prepared, studied, and structurally characterized

(18) Hunter, C. A. *Chem. Soc. Rev.* **1994**, *23*, 101.

(19) (a) Laarhoven, W. H.; Prinsen, W. J. C. In *Stereochemistry*; Vögtle, F., Weber, E., Eds.; Springer-Verlag: Berlin, 1984; p 63. (b) Janke, R. H.; Haufe, G.; Würthwein, E. U.; Borkent, J. H. *J. Am. Chem. Soc.* **1996**, *118*, 6031.

(20) Katzenelson, O.; Edelstein, J.; Avnir, D. *Tetrahedron: Asymmetry* **2000**, *11*, 2695.

by Steel and Caygill.[21] Its helicity in the solid state has been shown to stem from the steric repulsion operating on the two palladated phenyl groups connected at the 2- and 3-positions of the pyrazine ring. Actually, in solution, the latter pentacyclic Pd(II) complex is conformationally fluxional and exists under two swiftly exchanging and equally populated forms of helices of *M* and *P* handedness (in eq 3 the complex is drawn in

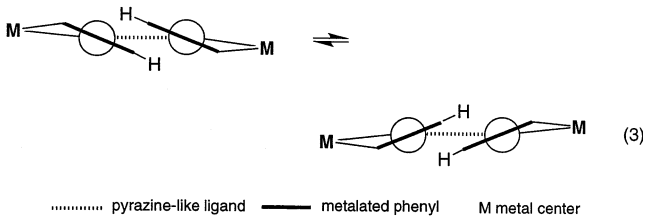

(3)

a Newman-type side view). As a consequence, such an achiral fluxional helical system may be qualified as being "pro-helical" rather than strictly helical.

It is worth noting that the introduction of factors of asymmetry in such a system could putatively modify the population of the two isomers in solution, thus enabling stereoselective reactions at the metal centers. The stereochemical course of any reaction occurring in the coordination sphere of each chelated metal should be conditioned by the intrinsic conformational and steric requirements of the substrate. As will be shown below, the bis-manganation of ligand **3a** affords a dinuclear complex **3b**, for which the structural features resemble those of the Pd(II) analogue mentioned above (eq 4). The

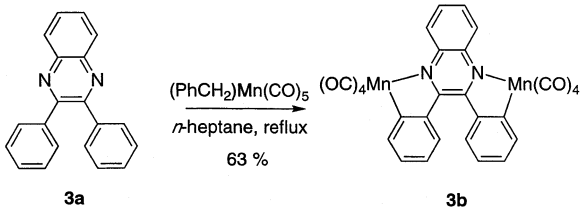

3a **3b** (4)

twisting of the two phenyl groups and by extension the "pro-helicity" of **3b** is expected to influence the stereochemical course of the reaction with the diazoalkane R_2CN_2. The sequential double addition of R_2CN_2 in an anti fashion (with respect to the mean plane of the chelate **3b)** is rather favored, as it results in an increase of the torsion angle between the planes of the two phenyl groups and the heterocycle, thus yielding a less sterically congested product (Scheme 2). A syn fashion double addition of the diazoalkane is disfavored, since it leads to a more sterically congested system (Scheme 2).

The bis-cyclomanganation of 2,3-diphenylquinoxaline **3a** was achieved by carrying out the reaction with $(PhCH_2)Mn(CO)_5$ at reflux of *n*-heptane. We observed that the reaction conditions should be slightly forced by reacting a concentrated mixture of a stoichiometric amount of $(PhCH_2)Mn(CO)_5$ (2 equiv) and **3a** over ca. 20 h, which contrasts with an earlier report by Bruce and co-workers,[22] who did not succeed in doubly ortho-

Scheme 2

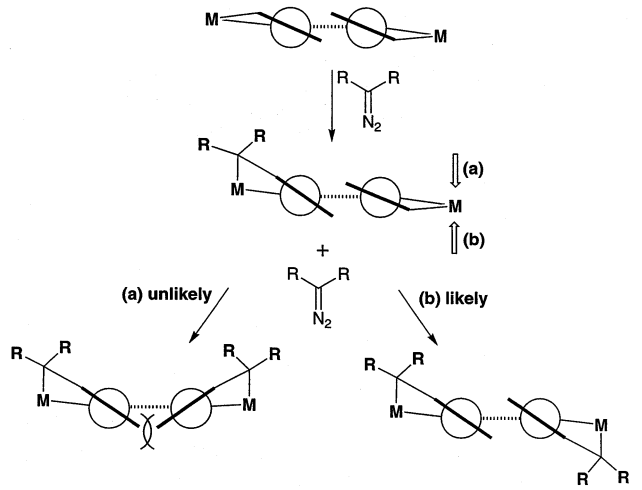

metalating this heterocyclic ligand, neither with $MeMn(CO)_5$ nor with $(PhCH_2)Mn(CO)_5$.

The purple dinuclear complex **3b** displayed good stability to air and reacted smoothly with an excess amount of Ph_2CN_2 in a mixture of boiling toluene and *n*-heptane (eq 5). Unexpectedly, the color of the medium

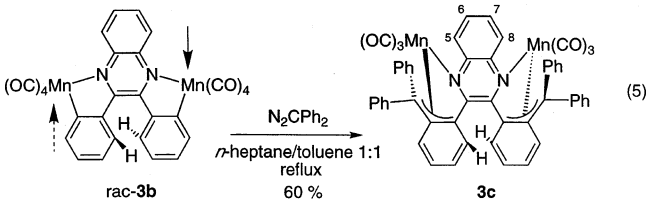

rac-**3b** **3c** (5)

quickly changed from deep purple to dark blue. The product, **3c**, was separated by conventional flash chromatography and recovered as an air-stable dark blue powder. Obtaining crystals suitable for X-ray diffraction analyses was complicated by the high solubility of **3c** in aliphatic nonpolar solvents. Only the slow evaporation of an *n*-heptane solution of **3c** at 4 °C afforded crystals of sufficient quality.

Figure 2 displays an ORTEP diagram of complex **3c** with the atom-numbering scheme. The structure of this binuclear complex indicates clearly that the reaction of the 2 equiv of Ph_2CN_2 took place on opposite faces of the substrate **3b**: in other words, in an anti fashion (eq 5). In complex **3c**, the heterocycle is embedded between the two endo phenyl rings (Figure 3). The stacking of the aromatic rings is characterized by interplanar angles of ca. 20° and distances between centroids of vicinal rings of ca. 3.4 Å (Figure 3). The phenylene rings are twisted by a value of ca. 50° with respect to the central heterocycle and are mutually involved in CH$-\pi$ interactions[23] via the hydrogen atoms located at C21 and C50, respectively. The distortion of an η^3 type bond involving the organic ligand and the two manganese(I) centers is similar to that previously encountered with other manganospiralenes. The distortion of the geometry of **3c** from ideal C_2 symmetry suggests some strains stemming from crystal packing.

(21) Steel, P. J.; Caygill, G. B. *J. Organomet. Chem.* **1990**, *395*, 359.
(22) Bruce, M. I.; Goodall, B. L.; Matsuda, I. *Aust. J. Chem.* **1975**, *28*, 1259.
(23) (a) Nishio, M.; Hirota, M.; Umezawa, Y. In *The CH/π Interaction, Evidence, Nature and Consequences*; Wiley-VCH: New York, 1998. (b) Umezawa, Y.; Tsuboyama, S.; Takahashi, H.; Uzawa, J.; Nishio, M. *Tetrahedron* **1999**, *55*, 10047.

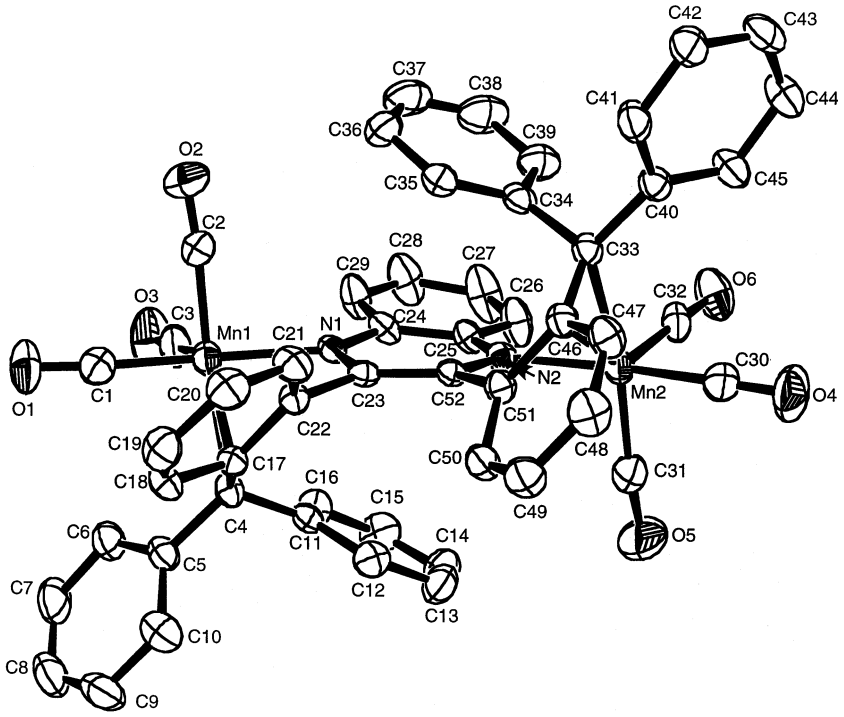

Figure 2. ORTEP diagram of complex **3c** displayed at the 30% probability level. Hydrogen atoms have been omitted for clarity purposes. Selected interatomic distances (Å): Mn1−N1, 2.057(3); Mn1−C4, 2.161(4); Mn1−C17, 2.203(3); Mn1−C22, 2.401(3); Mn2−N2, 2.043(3); Mn2−C33, 2.154(4); Mn2−C46, 2.220(3); Mn2−C51, 2.388(3). Torsion angle absolute value (deg): C22−C23−C52−C51, 8.5. Selected angles between mean planes P_1 (C34−C35−C36−C37−C38−C39), P_2 (N1−C23−C52−N2−C25−C26−C27−C28−C29−C24), P_3 (N1−C23−C52−N2−C25−C24), and P_4 (C51−C50−C49−C48−C47−C46) (deg): P_1−P_2, 22.3; P_3−P_4, 53.5. Distance between centroids, Cg_n, of planes P_n (Å): Cg_1−Cg_3, 3.43 Å.

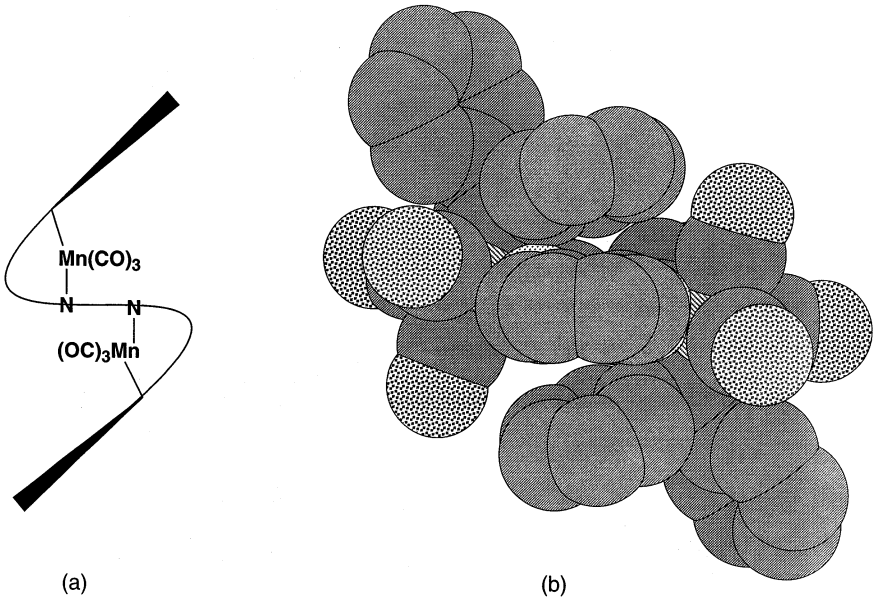

Figure 3. Representations of complex **3c**: (a) a sketch outlining the helical shape; (b) space-filling representation emphasizing the intramolecular stacking of aromatic rings.

Thermolytic Reaction of 9-Diazofluorene with *cis*-(LC)Mn(CO)$_4$ Complexes: New Method for the Synthesis of Appended η^5-Coordinated Fluorenyls. Diazocyclopentadienyl[24] and its indenyl[25a] and fluorenyl[25b] analogues have been intensively studied for their reactivity with transition-metal centers. As far as mononuclear rhenium carbonyl and manganese carbonyl type complexes are concerned, Herrmann and co-workers carried out the very first investigations in the 1970s.[12] The most recent achievements have been made in the late 1990s.[26] Katzenellenbogen and co-workers synthesized a variety of appended tricarbonyl(η^5-cyclopentadienyl)rhenium analogues as well as other tech-

(24) (a) Doering, W. v. E.; DePuy, C. H. *J. Am. Chem. Soc.* **1953**, *75*, 5955. (b) Weil, T.; Cais, M. *J. Org. Chem.* **1963**, *28*, 2472.

(25) (a) Rewicki, D.; Tuschcherer, C. *Angew. Chem.* **1972**, *84*, 31. (b) Pfeiffer, J.; Nieger, M.; Dötz, K. H. *Chem. Eur. J.* **1998**, *4*, 1843. (c) Pfeiffer, J.; Dötz, K. H. *Organometallics* **1998**, *17*, 4353. (d) Pfeiffer, J.; Dötz, K. H. *Angew. Chem.* **1997**, *109*, 2948; *Angew. Chem., Int. Ed. Engl.* **1997**, *36*, 2828. (e) Pfeiffer, J.; Nieger, M.; Dötz, K. H. *Eur. J. Org. Chem.* **1998**, 1011.

netium derivatives by an elegant "one pot" procedure consisting of a reaction between a $XL_3M(CO)_3$ complex (X = a one-electron ligand, L = a two-electron ligand), diazocyclopentadiene, $N_2C_5H_4$, and a "nucleophile", Nu, such as an arylboronic acid. In a comprehensive report[27] the authors demonstrated that the formation of the final appended $RCpM(CO)_3$ complex results from the reaction of $N_2C_5H_4$ with a putative $Nu-ML_3(CO)_3$ species via a transient metal−alkylidene intermediate. The latter evolves by cis migration of Nu on the carbene carbon to give a η^1-Cp intermediate, which undergoes a series of ring slippages to afford the final η^5-Cp complex. This multistep mechanism strongly resembles the one we have established for the formation of manganospiralenes[5] and confirms the major role played by transient alkylidene-type species.

We decided to study the behavior of *cis*-$(LC)Mn(CO)_4$ versus the readily available 9-diazofluorene, which can be made by oxidation of fluorene hydrazone with yellow HgO. For instance, the treatment of complex **1a** with 9-diazofluorene in a refluxing mixture of *n*-heptane and toluene afforded the heterobimetallic compound **1c** in 54% yields (eq 6). In this reaction the diazoalkane

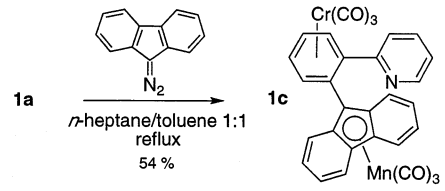

(6)

undergoes a competing decomposition into dimerization products,[28] which can challenge the C−C coupling reaction with the cyclometalated substrate. The procedure was optimized significantly by using mixtures of aliphatic solvents and toluene and by reacting ca. 2 equiv of diazoalkane in a boiling solution containing the starting complex. The course of the reaction could be monitored by IR spectroscopy. The experiment was stopped when the IR measures indicated the disappearance of the characteristic four CO stretching bands of the $Mn(CO)_4$ fragment of the substrate and the clear appearance of two new CO stretching bands corresponding to a typical *fac*-$L_3M(CO)_3$ species beside the two CO stretching bands originating from the $Cr(CO)_3$ group. The change in color of the reaction medium was also a good indicator of the rate of the reaction. In the case of the reaction of **1a** with 9-diazofluorene, the color of the medium changed from deep red to canary yellow in ca. 30 min. The product, e.g. complex **1c**, could be successfully recrystallized to afford a suitable sample for X-ray diffraction analyses. Figure 4 presents an ORTEP diagram of compound **1c**.

In Figure 4, one can notice the particular arrangement of the two metal-bound aromatic rings represented

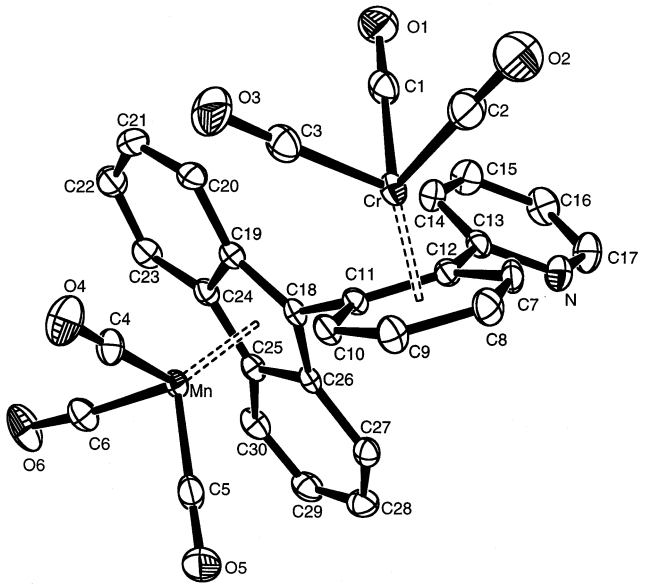

Figure 4. ORTEP diagram of complex **2c** given at the 40% probability level. Hydrogen atoms have been omitted for clarity purposes. Selected interatomic distances (Å): Cr−C12, 2.229(3); Cr−C11, 2.260(3); Cr−C10, 2.212(3); Cr−C9, 2.215(3); Cr−C8, 2.207(3); Cr−C7, 2.206(3); Mn−C18, 2.137(3); Mn−C19, 2.180(3); Mn−C24, 2.197(3); Mn−C25, 2.198(3); Mn−C26, 2.199(3). Metal to plane centroid distances (π-coordinated ligands) (Å): Mn−Cg, 1.8051(14); Cr−Cg, 1.7168(13). Selected angles between mean planes P_1 (C12−C11−C10−C9−C8−C7), P_2 (N−C13−C14−C15−C16−C17), and P_3 (C18−C19−C24−C25−C26) (deg): P1−P2, 77.4; P2−P3, 38.8.

by the corresponding planes P_1(C11−C12−C7−C8−C9−C10) and P_3(C18−C19−C24−C25−C26); the corresponding interplanar angle P_1-P_3 is 77.4°. The nitrogen atom of the pyridyl fragment points outward, probably as a result of an electrostatic repulsion with the π system of the vicinal fluorenyl group. This effect added to the hindrance caused by the 1,2-substitution pattern of the Cr-bound phenylene group disables a trans relationship between the two $M(CO)_3$ fragments, as observed by Quian[29] in a similar but less hindered case.

Scheme 3 rationalizes the mechanism of formation of **1c**. The first step is the departure of one molecule of CO from the starting $M(CO)_4$ moiety and its replacement by the Fischer-type electrophilic alkylidene fragment. The second step is the cis migration of the aryl group bonded to the central metal atom and the formation of a labile Mn(I) chelate that can readily undergo several haptotropic shifts and rearrangements between various η^3 bonding modes (vide infra). The key step is clearly the cleavage of the N−Mn bond. The driving force of the overall process is the formation of a stable (η^5-fluorenyl)$Mn(CO)_3$ species.

Complex **2a** reacted similarly with 9-diazofluorene (eq 7). The reaction was carried out in pure refluxing

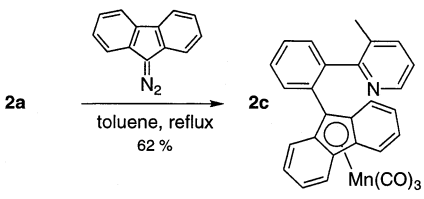

(7)

toluene and afforded the polar (η^5-fluorenyl)$Mn(CO)_3$

(26) (a) Minutolo, F.; Katzenellenbogen, J. A. *J. Am. Chem. Soc.* **1998**, *120*, 13264. (b) Spradau, T. W.; Katzenellenbogen, J. A. *Organometallics* **1998**, *17*, 2009. (c) Minutolo, F.; Katzenellenbogen, J. A. *Angew. Chem.* **1999**, *111*, 1730. (d) Cesati, R. R.; Katzenellenbogen, J. A. *J. Am. Chem. Soc.* **2001**, *123*, 4093. (e) For a case involving $Re_2(CO)_8(MeCN)_2$ see: Arce, A. J.; Muchado, R.; De Sanctis, Y.; Isea, R.; Atencio, R.; Deeming, A. J. *J. Organomet. Chem.* **1999**, *580*, 339.

(27) Minutolo, F.; Katzenellenbogen, J. A. *Organometallics* **1999**, *18*, 2519.

(28) Bertani, R.; Michelin, R. A.; Mozzon, M.; Sassi, A.; Basato, M.; Biffis, A.; Martinati, G.; Zecca, M. *Inorg. Chem. Commun.* **2001**, *4*, 281.

species appended with a 2-(3′-methylpyridin-2′-yl)phenyl group, e.g. **2c**, in 62% yield. The chiral complex **4a**[4] reacted readily with 9-diazofluorene (eq 8) to give in 85%

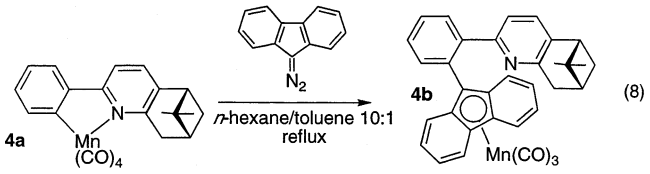

(8)

yield the corresponding (η^5-fluorenyl)$Mn(CO)_3$ derivative, whose chirality was evidenced by polarimetry ($[\alpha]_D$-(293 K) = $-33 \pm 1°$ dm^{-1} g^{-1} mL).

The cyclorhenated complex **5a**[6c] also reacted with 9-diazofluorene (eq 9). The reaction was slower than in

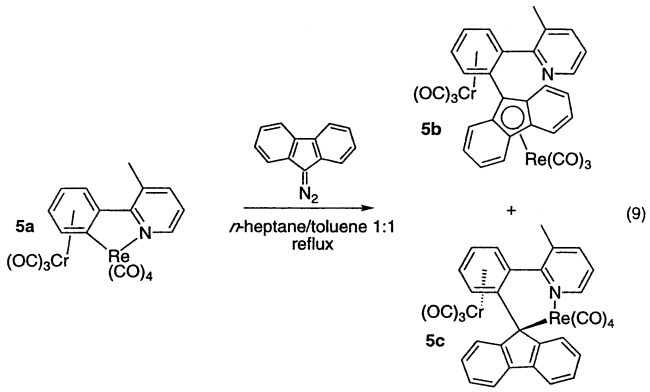

(9)

the case of the manganese analogue **1a**. In fact, not only did the experiment require longer reaction times to reach optimum conversion, but also the medium underwent some decomposition and the overall conversion was quite low. Chromatographic separation of the crude mixture afforded minute amounts of the starting complex and delivered two new reaction products. The structures of the last two compounds (eq 9), **5b**,**c**, were assessed firmly only after analyses of their respective ^{13}C NMR spectra and the X-ray diffraction analysis of a crystal of **5c**. Figure 5b displays the structure of complex **5c**, and Figure 5a presents an unprecedented ORTEP diagram of substrate **5a**, which is given for comparison purposes. The structure of complex **5a** is typical of cyclorhenated aromatics. The molecule, which possesses no peculiar distortions, presents geometrical trends that are similar to those of known Mn(I) analogues. The particularly long Cr−C8 interatomic distance of 2.334(3) Å mostly arises from the steric hindrance created by the $Re(CO)_4$ fragment. The aromatic rings are slightly twisted by a value of 16.2° for the corresponding torsion angle C8−C7−C1−N. In complex **5c** (Figure 5b), the two metal carbonyl fragments are positioned anti to each other. The coordination environment about the rhenium atom is nearly octahedral. The six-membered metallacycle consisting of atoms Re−C13−C11−C6−C5−N adopts a folded envelope-like conformation. The valence angles around atom C13 do not fully fit the standard features of a carbon sp^3 type hybridization, although the Re−C13 distance of 2.357(4) Å corresponds to that of a single $Re-C_{Cp}$ bond distance (2.360(10) Å) found, for instance,

Scheme 3

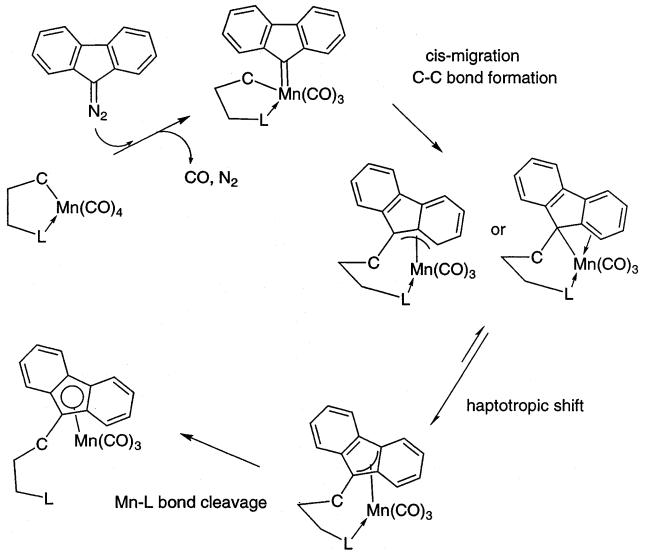

with *fac*-(η^1-C_5H_5)$Re(CO)_3(PMe_3)_2$.[30] Intramolecular cluttering caused by the $Re(CO)_4$-bound ligand accounts for the particularly long Cr−C11 distance of 2.337(4) Å.

On the basis of our experience of the chemistry of Mn(I) and Re(I) chelates, we thought it unlikely that compound **5c** could arise from a direct homolytic cleavage of the C_{Ar}−Re bond in **5a** followed by a coupling with some "alkylidenoid" species. We carried out an additional experiment aiming at proving that complex **5c** stems from a reaction of **5b** with dissolved CO. Such a hypothesis would imply that formation of **5c** results from successive haptotropic shifts of the fluorenyl-bound rhenium center upon coordination of both endogenous and exogenous ligands. Such processes are well documented for $CpM(CO)_3$-type complexes (M = Mn, Re).[31]

A concise mechanistic proposal is provided in Scheme 4. In a first step, the endogenous ligand L coordinates the Re center and induces an $\eta^5-\eta^3$ haptotropic shift. In a second step, the intermediate equilibrates with a η^1-type isomer, presenting a vacant coordination site. Dissolved carbon monoxide arising from the decomposition of some reactive species bonds to the rhenium atom in the last step to give the chelated *cis*-(LC)$Re(CO)_4$ product. This proposal was checked by submitting a solution of **5b** to heat under an atmosphere of CO. Within a few minutes, IR spectral analysis of the reaction mixture indicated the conversion of **5b** into **5c**

(29) Quian, C.; Guo, J.; Sun, J.; Chen, J.; Zheng, P. *Inorg. Chem.* **1997**, *36*, 1286.

(30) Casey, C. P.; O'Connor, J. M.; Jones, W. D.; Haller, K. J. *Organometallics* **1983**, *2*, 535.

(31) (a) Stradiotto, M.; McGlinchey, M. J. *Coord. Chem. Rev.* **2001**, *219−221*, 311. (b) Casey, C. P.; Kraft, S.; Powell, D. R. *Organometallics* **2001**, *20*, 2651. (c) Abernethy, C. D.; Cowley, A. H.; Jones, R. A.; Macdonald, C. L. B.; Shukla, P.; Thompson, L. K. *Organometallics* **2001**, *20*, 3629. (d) Veiros, L. F. *Organometallics* **2000**, *19*, 5549. (e) Khayatpoor, R.; Shapley, J. R. *Organometallics* **2000**, *19*, 2382. (f) Lee, S.; Lovelace, S. R.; Cooper, N. J. *Organometallics* **1995**, *14*, 1974. (g) Biagioni, R. N.; Luna, A. D.; Murphy, J. L. *J. Organomet. Chem.* **1994**, *476*, 183. (h) Treichel, P. M.; Johnson, J. W. *Inorg. Chem.* **1977**, *16*, 749. (i) Lee, S.; Cooper, N. J. *J. Am. Chem. Soc.* **1991**, *113*, 716. (j) Casey, C. P.; O'Connor, J. M. *Chem. Rev.* **1987**, *87*, 307. (k) Basolo, F.; Rerek, M. E.; Ji, L. N. *Organometallics* **1984**, *3*, 740. (l) Yezernitskaya, M. G.; Lokshin, B. V.; Zdanovich, V. I.; Lobanova, I. A.; Kolobova, N. E. *J. Organomet. Chem.* **1982**, *234*, 329. (m) Casey, C. P.; O'Connor, J. M. *Organometallics* **1985**, *4*, 384. (n) King, R. B.; Efraty, A. *J. Organomet. Chem.* **1970**, *23*, 527. (o) Casey, C. P.; Kraft, S.; Kavana, M. *Organometallics* **2001**, *20*, 3795.

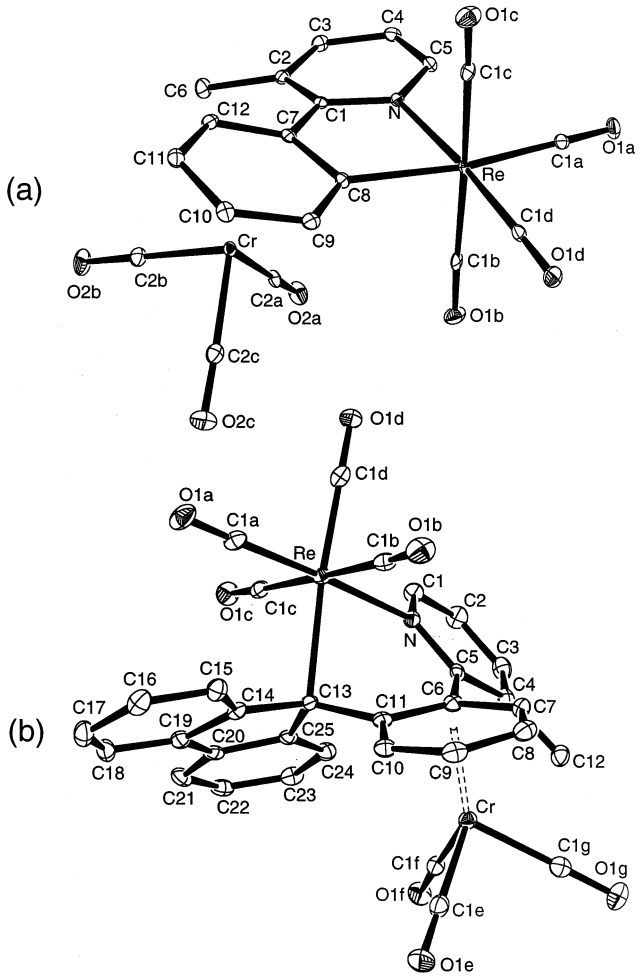

Figure 5. (a) ORTEP diagram of complex **5a** given at the 30% probability level. Hydrogen atoms have been omitted for clarity purposes. Selected interatomic distances (Å): Cr−C7, 2.207(3); Cr−C8, 2.334(3); Cr−C9, 2.259(3); Cr−C10, 2.201(3); Cr−C11, 2.211(3); Cr−C12, 2.201(3); Re−C8, 2.169(3); Re−N, 2.202(2). Selected interatomic angles (deg): C9−C8−C7, 117(3); C8−Re−N, 75.73(10). Selected torsion angles (deg): C8−C7−C1−N, 16.2(4); C1−C7−C8−Re, 10.7(3). (b) ORTEP diagram of complex **5c** given at the 30% probability level. Hydrogen atoms have been omitted for clarity purposes. The geometrical data of one molecule of the asymmetric unit are given. Selected interatomic distances (Å): Re1−N1, 2.227(3); Re1−C13, 2.357(4); Cr1−C6, 2.266(4); Cr1−C7, 2.206(4); Cr1−C9, 2.189(4); Cr1−C10, 2.202(4); C11−C13, 1.505(6). Metal-to-centroid distance (Å): Cr1−Cg, 1.725(3). Selected interatomic bond angles (deg): C25−C13−C14, 102.2(3); C10−C11−C6, 115.8(4). Selected values of absolute torsion angles (deg): N1−C5−C6−C11, 44.4(6); C5−C6−C11−C13, 3.8(6).

and the presence of some other minor species that could not be identified. Furthermore, we observed that, upon cooling and replacement of the CO blanket by argon, the medium would evolve to afford the starting complex **5b**. This result conspicuously confirms that the decomposition process taking place in the reaction between **5a** and 9-diazofluorene actually provides the carbon monoxide that is incorporated into **5b** to give **5c**. To the best of our knowledge, complex **5c** represents one new case of rhenium(I) complex in which the fluorenyl ligand is η^1-bonded to the metal center.

Synthesis of an Organometallic Quinoxaline: A Fluxional Helix Locked by Inclusion into a Coordination Polymer. Complex **3b** was treated with 9-diazofluorene to subsequently afford the new bimetallic product **3d** (Scheme 5). The reaction was carried out in pure toluene, and **3d** was recovered in 79% yield after chromatographic purification. A color change from deep purple to canary yellow took place within the few minutes that followed the addition of 2 equiv of 9-diazofluorene. We recrystallized **3d** and submitted a crystal to X-ray diffraction analysis. An ORTEP diagram of **3d** is presented in Figure 6.

Scheme 4

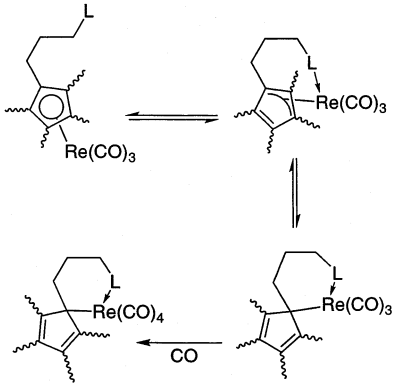

Scheme 5

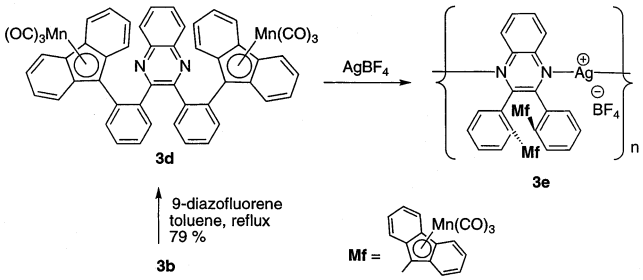

The structure of **3d** is clearly helical in shape as a result of the compact arrangement of the three central 1,2-disubstituted aromatics. The two $Mn(CO)_3$ moieties point outward to minimize steric interactions and allow stabilizing intramolecular $\pi-\pi$ stacking. The overall "molecular compactness" can be described by the intramolecular $\pi-\pi$ contacts existing between the free face of the two (η^5-fluorenyl)$Mn(CO)_3$ groups and the two phenylene fragments. In the crystal lattice, **3d** is packed in a columnar fashion, intermolecular interaction being established between $Mn(CO)_3$ moieties of each molecule. As can be noticed in Figure 6, a quite cluttered environment surrounds the two nitrogen atoms of the heterocycle. The geometry of **3d** deviates slightly from the ideal C_2-type symmetry. These discrete distortions consist of slight twists and folding such as the dihedral angle C25−C26−C29−C34, which amounts to 3.1°.

Quinoxalines, pyrazines, and other bis-monodentate ligands based on two interconnected pyridine rings are often used in the synthesis of inorganic−organic hybrid polymers,[32] applied in crystal engineering and derived in the synthesis of electroluminescent organic polymers. When silver cation is used as the "cement", these ligands are also appropriate synthons for the construction of single-strand linear hybrid inorganic/organic polymers and even more sophisticated supramolecular assem-

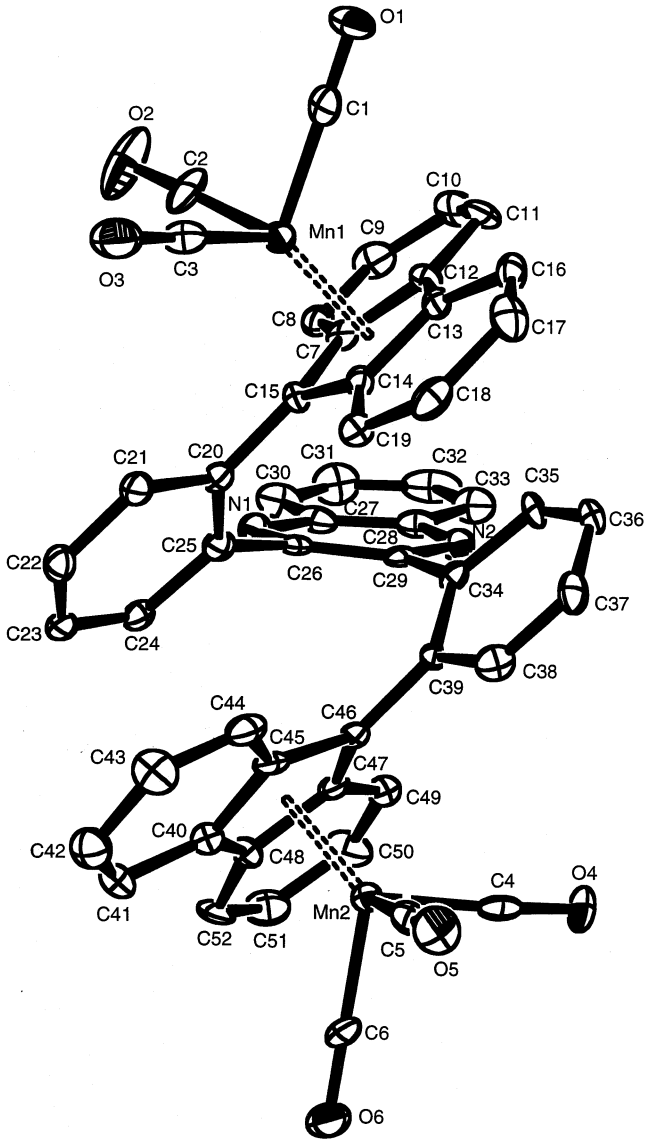

Figure 6. ORTEP diagram of complex **3d** given at the 40% probability level. Molecules of solvent and hydrogen atoms have been omitted for clarity purposes. Selected interatomic distances (Å): Mn1−C15, 2.147(8); Mn1−C7, 2.190(7); Mn1−C14, 2.201(7); Mn1−C13, 2.207(7); Mn1−C12, 2.233(7). Selected interatomic angles (deg): C14−C15−C7, 105.5(6); C15−C14−C13, 110.5(6); C14−C13−C12, 106.8(7); C13−C12−C7, 107.9(6). Absolute value of torsion angle C25−C26−C29−C34 (deg): 3.1(12).

blies.[33] As shown in Figure 6, complex **3d** contains a quinoxaline nucleus shielded by the two (η^5-fluoren-9-yl)$Mn(CO)_3$ fragments. Of course, such a conformation must be considered as a limit, since free rotation of these aromatic fragments is allowed in solution (Scheme 6). It is understood that one given (η^5-fluorenyl)$Mn(CO)_3$ group changes its position only in synergy with the other one, in a so-called flip-flop movement (Scheme 6). To

Scheme 6

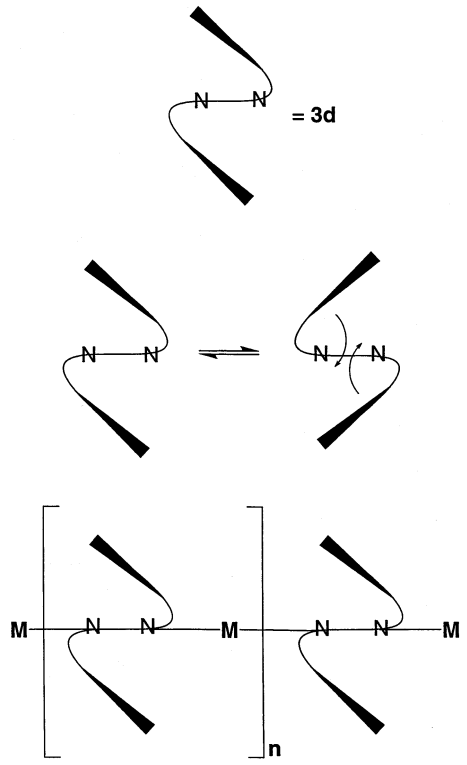

stabilize the helical architecture and gain a higher conformational stability, the dynamic conformational change has to be restricted by dramatically increasing the energetic barrier to interconversion. With **3d**, this can be achieved by locking the molecular helix through an increase of the degree of substitution at the two nitrogen atoms of the central heterocycle, either by current methods of organic chemistry, i.e., by bisalkylation of the two N atoms, or by means of coordination chemistry methods, i.e., by bonding these heteroatoms to the electrophilic metal "M" (Scheme 6).

We chose the second method. In our hands, the reaction of **3d** with stoichiometric amounts of $AgBF_4$ in acetone cleanly afforded, after slow crystallization, a new bright red linear hybrid inorganic/organometallic polymer **3e** (Scheme 5). The latter displayed a reasonable stability to air. Surprisingly, in this reaction we did not notice any decomposition of **3d** that could have been initiated by the known oxidizing properties of Ag^+ salts. Slow recrystallization of a crude sample of **3e** from a THF/MeOH solution by diffusion in *n*-heptane afforded crystals suitable for the X-ray diffraction analysis. An ORTEP diagram of **3e** is displayed in Figure 7 with a detailed atom-numbering scheme.

Polymer **3e** crystallizes in the noncentrosymmetric space group $P2_12_12_1$. In the analyzed crystal of **3e**, each local coordinated helix is of *M* handedness. Figure 7 shows an emphasized view of one polymeric single strand with the atom-numbering scheme. Similarly to

(32) (a) Schmaltz, B.; Jouaiti, A.; Hosseini, M. W.; De Cian, A. *Chem. Commun.* **2001**, 1242. (b) Fitchett, C. M.; Steel, P. J. *New J. Chem.* **2000**, *24*, 945. (c) Maggard, P. A.; Stern, C. L.; Poeppelmeier, K. R. *J. Am. Chem. Soc.* **2001**, 123, 7742. (d) Bourne, S. A.; Kilkenny, M.; Nassimbeni, L. R. *J. Chem. Soc., Dalton Trans.* **2001**, 1176. (e) Hartmann, H.; Berger, S.; Winter, R.; Fiedler, J.; Kaim, W. *Inorg. Chem.* **2000**, *39*, 4977. (f) Blake, A. J.; Champness, N. R.; Crew, M.; Parsons, S. *New J. Chem.* **1999**, 13. (g) Blake, A. J.; Champness, N. R.; Khlobystov, A. N.; Lemenovskii, D. A.; Li, W. S.; Schröder, M. *Chem. Commun.* **1997**, 1339.

(33) (a) Khlobystov, A. N.; Blake, A. J.; Champness, N. R.; Lemenovskii, D. A.; Majouga, A. G.; Zyk, N. V.; Schröder, M. *Coord. Chem. Rev.* **2001**, 222, 155. (b) Munakata, M.; Wu, L. P.; Ning, G. L. *Coord. Chem. Rev.* **2000**, *198*, 171. (c) Klein, C.; Graf, E.; Hosseini, M. W.; De Cian, A. *New J. Chem.* **2001**, *25*, 207. (d) Loï, M.; Hosseini, M. W.; Jouaiti, A.; De Cian, A.; Fischer, J. *Eur. J. Inorg. Chem.* **1999**, 1981. (e) Kaes, C.; Hosseini, M. W.; Rickard, C. E. F.; Skelton, B. W.; White, A. H. *Angew. Chem.* **1998**, *110*, 970; *Angew. Chem., Int. Ed. Engl.* **1998**, *37*, 920.

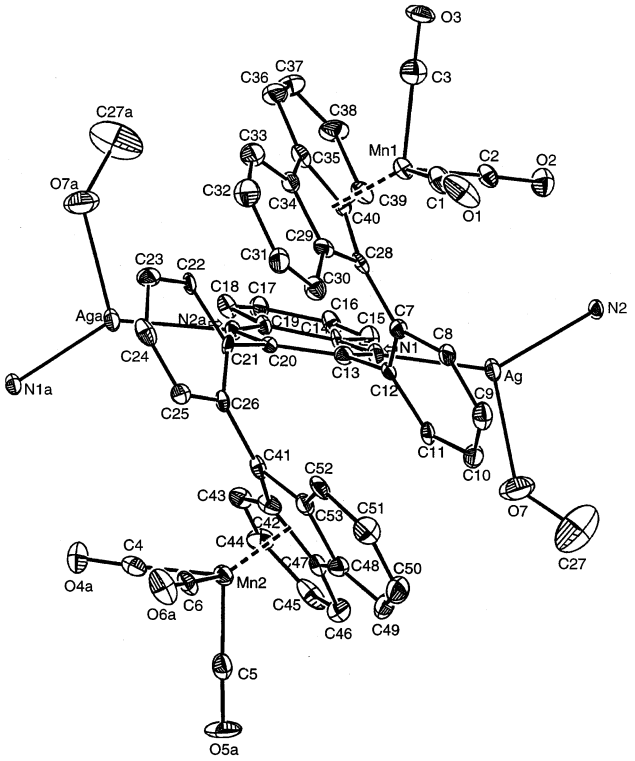

Figure 7. ORTEP diagram of a unit of polymer **3e** drawn at the 20% probability level. The solvated MeOH molecule, disordered BF_4^- molecule, and hydrogen atoms have been omitted for clarity purposes. Selected interatomic distances (Å): Ag−N1, 2.251(9); Ag−N2, 2.281(9); Ag−O7, 2.32(1); Mn1−C28, 2.14(1); Mn1−C29, 2.19(1); Mn1−C34, 2.19(1); Mn1−C35, 2.22(1); Mn1−C40, 2.19(1); Mn2−C42, 2.19(1). Selected valence angles (deg): N1−Ag−N2, 141.3(3); N1−Ag−O7, 109.4(4); N2−Ag−O7, 109.2(4); C29−C28−C40, 106(1). Selected absolute torsion angle (deg): C21−C20−C13−C12, 3.4(14); C20−C21−C28−C41, 1.3(16). Selected angles between mean planes P_1 (C20−C13−C19−C14−N1−N2a), P_2 (C7−C12−C11−C10−C9−C8), P_3 (C28−C29−C34−C35−C40), P_4 (C21−C22−C23−C24−C25−C26) (deg): P_3-P_4, 12.8; P_2-P_4, 56.9; P_3-P_2, 44.9; P_1-P_2, 57.1. Selected distances between centroids of corresponding planes (Å): Cg3-Cg4, 3.59; Cg3-Cg1, 4.66.

3d, in each subunit of the polymer, the pentacyclic ligand adopts the shape of an helix. The polymer is not strictly linear, as can be seen in Figure 8. Indeed, coordination of one molecule of MeOH per silver atom induces a zigzag shape, which is often observed with other Ag^+-based coordination polymers. This red polymer was analyzed by IR spectroscopy: a spectrum taken with a KBr pellet sample of **3e** displayed no difference from a reference spectrum of **3d** measured under the same conditions, thus suggesting there is no significant effect of the coordinated silver atom on the electron density at the manganese atoms.

The above-mentioned results motivate us now to closely investigate the synthetic application of such a new carbon−carbon bond-forming reaction, to address the reactivity of other cyclomanganated complexes versus diazocyclopentadiene derivatives, and to study the chemical properties of this new class of appended $CpMn(CO)_3$-like complexes for which a few examples have already been reported.[34] For instance, the reaction of the acetophenone derivative **6a**[35] with 9-diazofluorene affords a new (η^5-fluorenyl)$Mn(CO)_3$ complex appended

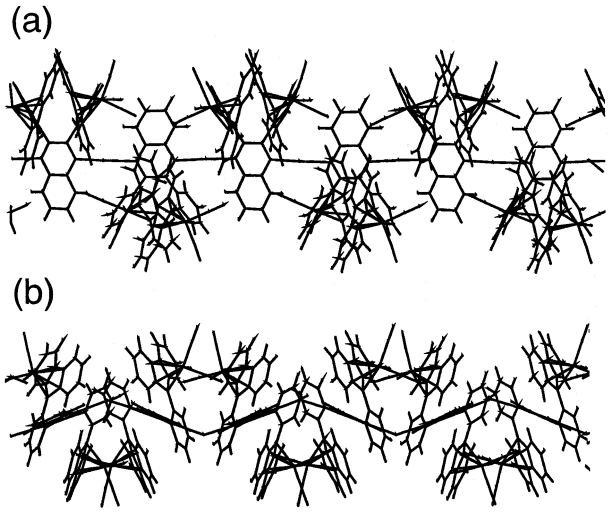

Figure 8. Stick-type diagram displaying a portion of a strand of the hybrid inorganic−organometallic polymer **3e**: (a) view from the top, showing the alternating quinoxaline rings in a "head-to-tail" configuration; (b) view from the side, showing the zigzag shape conferred to the polymeric chain by the coordination of one molecule of MeOH (not shown) to the Ag center. The solvated MeOH as well as disordered BF_4^- have been omitted for clarity purposes.

with a 2-acetylphenyl fragment at the 9 position, e.g. **6b** in 82% yield (eq 10). Further advances on this topic shall be disclosed in due time.

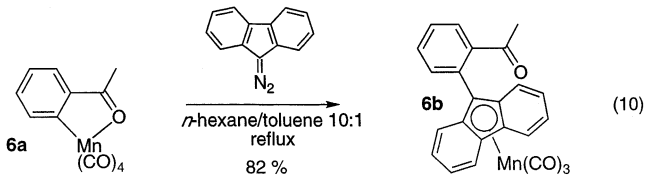

(10)

Electrochemical Behavior of Manganospiralenes. The electrochemical properties of several spiralenes were studied by cyclic voltammetry in CH_3CN and THF, using mostly a polished flat Pt-bead working electrode. Electrochemical data are reported in Table 2. Complexes **1b**, **2b**, and **7**−**11** (Chart 1) all displayed only one reversible reduction wave at potentials higher than −1.8 V vs SCE (saturated calomel electrod), while oxidation proved to be in most cases irreversible electrochemically, likely as a result of a metal-centered ECE-type process (Table 2).[36] Anodic/cathodic peak-potential separations for the processes related to reduction in cyclic voltammetry experiments were found to depend on the nature of both the working electrode and the solvent. Smaller ΔE ($\Delta E = E_{p,c} - E_{p,a}$) values, e.g. close to the value of 59 mV for a monoelectronic process, could be obtained with a hanging-Hg-drop working electrode. The high values of ΔE obtained with a Pt-bead electrode can be related to uncompensated solution resistance and to

(34) (a) Top, S.; Kaloun, E. B.; Toppi, S.; Herrbach, A.; McGlinchey, M. J.; Jaouen, G. *Organometallics* **2001**, 20, 4554 and references therein. (b) Le Bideau, F.; Salmain, M.; Top, S.; Jaouen, G. *Chem. Eur. J.* **2001**, *7*, 2289. (c) Enders, M.; Kohl, G.; Pritzkow, H. *J. Organomet. Chem.* **2001**, *622*, 66.

(35) (a) McKinney, R. J.; Firestein, G.; Kaesz, H. D. *Inorg. Chem.* **1975**, *14*, 2057. (b) Knobler, C. B.; Schreiber-Crawford, S.; Kaesz, H. D. *Inorg. Chem.* **1975**, *14*, 2062.

(36) Herschberger, J. W.; Amatore, C.; Kochi, J. K. *J. Organomet. Chem.* **1983**, *250*, 345.

Table 2. Characterization of Various Spiralenes and Analogues by Cyclic Voltammetry

	Pt-bead working electrode, acetonitrile			Pt-bead working electrode, THF			Hg hanging drop working electrode, acetonitrile
compd	$E_{1/2}$(redn) (ΔE)	scan rate	E(oxidn)	$E_{1/2}$(redn) (ΔE)	scan rate	E(oxidn)	$E_{1/2}$(redn) (ΔE)
1b	−1.58 (0.33)			−1.67 (0.12)	100		
2b							−1.04 (0.06)[d]
3c	−0.93 (0.16)	100	+0.78[b]	−0.90 (0.11)	200		
	−1.69 (0.11)		+1.04[b]	−1.83 (0.12)			
3d	−1.56[b]	100	+1.01[b]				
			+1.19[b]				
7	−1.39 (0.95)	100	+0.72[b]	−1.43 (0.23)	200		
8	−1.56 (0.99)	100					
9	−1.37 (0.10)	100					−1.04 (0.07)[c]
10	−1.69[b]	400		−1.56 (0.17)	200	+0.75[b]	
11	−1.61 (0.17)	100	+0.24[b]				

[a] Potentials are expressed in V vs SCE and scan rates in mV s^{-1}. [b] Slow or nonreversible system. [c] Scan rate 200 mV s^{-1}. [d] Scan rate 100 mV s^{-1}.

Chart 1

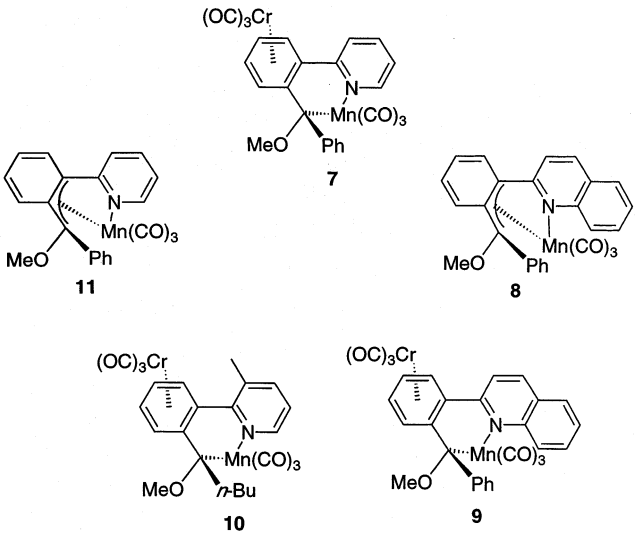

partial adsorption of reduced species on the surface of the Pt electrode. However, at this stage of our study, we cannot rule out the possible existence of underlying ECE processes similar to those evidenced by Amatore, Ceccon, and co-workers[37] with a parent system, i.e., syn- and anti-facial {μ-(1,2,3,4,5,6-η:7,8,9-η)]-indenyl}$(CO)_3$Cr−Rh(cod) complexes. Most measures carried out with heterobinuclear spiralenes displayed in reduction the classical behavior of reversible systems though. In all cases, the variation of the peak current associated with the reduction wave(s) with the scan rate was that of a reversible electrochemical system.

Interestingly, complex **3c** displayed at room temperature in THF two electrochemically reversible reduction waves at −0.90 and −1.83 V vs SCE (Figure 9a) similarly to unsubstituted quinoxaline in DMF as reported by Mubarak and Peters.[38a] This contrasts with the behavior of 2,3-diphenylquinoxaline, which is known to undergo only one-electron reversible reduction at −1.63 V vs SCE.[38b] It is worthy to note that further reduction of 2,3-diphenylquinoxaline at a more negative cathodic potential leads to a reactive dianion, which irreversibly evolves by a C−C coupling reaction to yield the corresponding dibenzo[*a*,*c*]phenazine dianion.[39] Similarly, 2-ferrocenyl-3-phenylquinoxalines undergo an irreversible two-electron-reduction process leading to untraceable products.[40]

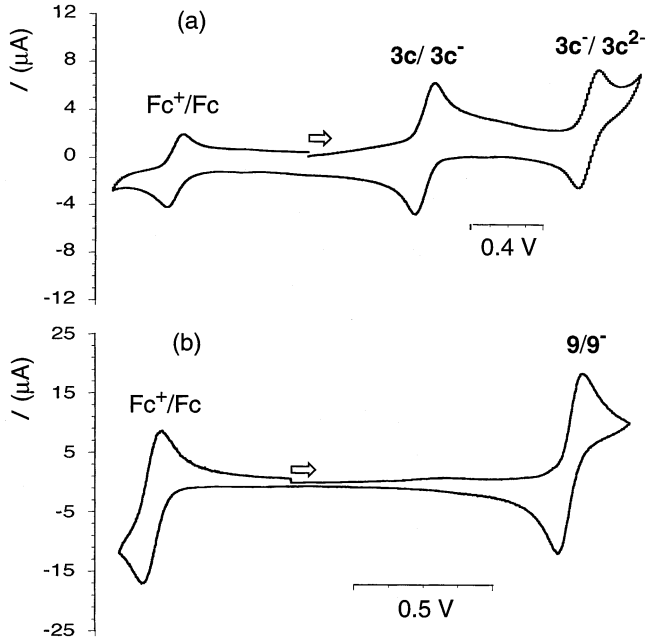

Figure 9. Cyclic voltammetry of spiralenes at room temperature (Pt-bead working electrode, Pt-wire counter electrode, Ag-wire pseudo reference electrode, a 0.1 N solution of $(n\text{-Bu})_4NPF_6$ as support electrolyte): (a) voltammogram of a THF solution of complex **3c** containing ferrocene as internal reference (1.66×10^{-4} M, 200 mV s^{-1}); (b) voltammogram of a solution of complex **9** in CH_3CN (2.50×10^{-3} M, 100 mV s^{-1}) containing ferrocene as internal reference.

By carrying out controlled-potential electrolysis experiments and cyclic voltammetry-based titrations with solutions of compounds **8** and **3c** in CH_3CN at room temperature, we could ascertain that the spiralene's reduction process involved the transfer of one electron. Complexes **3c** and **8** were reduced at a spiral-shaped Pt wire at −1.20 and −1.60 V vs SCE, respectively. For the electrolysis of **8** in CH_3CN the decay of the cathodic current as a function of time followed the expected exponential decay (see the Supporting Information). The transfer of one electron per molecule (0.25 C) of **8** was

(37) Amatore, C.; Ceccon, A.; Santi, S.; Verpeaux, J. N. *Chem. Eur. J.* **1999**, *5*, 3357.
(38) (a) Mubarak, M. S.; Peters, D. G. *J. Electroanal. Chem.* **2001**, *507*, 110. (b) Bock, H.; John, A.; Näther, C.; Ruppert, K. *Helv. Chim. Acta* **1994**, *77*, 1505.
(39) Rabinovitz, M.; Cohen, Y.; Meyer, A. Y. *J. Am. Chem. Soc.* **1986**, *108*, 7039.
(40) Zanello, P.; Fontani, M.; Ahmed, S. Z.; Glidewell, C. *Polyhedron* **1998**, *17*, 4155.

complete, under these conditions, after ca. 580 s of electrolysis. After this period of time a slight increase of the cathodic current was observed, which was symptomatic of the degradation of the radical anion $\mathbf{8}^-$. A similar experiment carried out with 4.38×10^{-3} mmol of **3c** led to the observation of a complete transfer of one electron per molecule of **3c** (0.42 C) after ca. 1000 s of electrolysis.

A complementary comparative cyclic voltammetry was carried out with a solution of **8** (3.32×10^{-3} M) using the hexafluorophosphate salt of methyl viologen ($c(PQ^{2+},2PF_6^-) = 2.62 \times 10^{-3}$ M) as a reference. The latter displays two consecutive one-electron reversible redox processes.[41] The values of the ratios $I_{p,c}/I_{p,a}$ for the two couples PQ^{2+}/PQ^+ and PQ^+/PQ corresponding to the two one-electron processes were estimated, within experimental errors, as 1.2 and 1.0, respectively. A value of 1.0 for the $I_{p,c}/I_{p,a}$ ratio of the couple $\mathbf{8}/\mathbf{8}^-$ was also determined (see the Supporting Information). A solution of a mixture of **8** and $PQ^{2+},2PF_6^-$ (ratio of concentrations $c(PQ^{2+},2PF_6^-)/c$ (**8**) = 0.79) afforded the value of 0.80 for the two ratios of cathodic peak currents $I_{p,c}(PQ^{2+}/PQ^+)/I_{pc}(\mathbf{8}/\mathbf{8}^-)$ and $I_{p,c}(PQ^+/PQ)/I_{pc}(\mathbf{8}/\mathbf{8}^-)$, thus further supporting the notion that reduction of **8** involves one electron.

In the heterobimetallic Cr(0)/Mn(I) complexes **7** and **9** the potentials of couples $\mathbf{7}/\mathbf{7}^-$ and $\mathbf{9}/\mathbf{9}^-$ are more positive by a value of ca. 190 mV than for those of the corresponding mononuclear analogues $\mathbf{11}/\mathbf{11}^-$ and $\mathbf{8}/\mathbf{8}^-$. This increase in potential can be intuitively correlated to the known electron-accepting properties of the $Cr(CO)_3$ moiety or interpreted by a significant lowering of the energy of the LUMO, which with likelihood is centered at the heterocyclic ligand of the considered binuclear species. It must be recalled that typical (η^6-arene)$Cr(CO)_3$ complexes undergo irreversible two-electron-reduction processes, yielding a reactive diamagnetic dianion.[42]

Reduction of 3c. In acetonitrile, the reduction of **3c** affords successively the radical anion $\mathbf{3c}^-$ ($E = -0.93$ V) and the anion $\mathbf{3c}^{2-}$ ($E = -1.69$ V), as demonstrated before by cyclic voltammetry. This behavior is reminiscent of that observed in mixed-valence compounds[43] that incorporate a pyrazine unit as bridge between two metallic ions or radicals in identical environments. The issues related to spin density localization and an analogy with the so-called mixed-valence species were preliminarily addressed by determining the comproportionation constant K_C for the process

$$\mathbf{3c} + \mathbf{3c}^{2-} \rightleftarrows 2\ \mathbf{3c}^-$$

($K_C = 10^{\Delta E/0.059}$, with ΔE in V) from the electrochemical potentials of couples $\mathbf{3c}/\mathbf{3c}^-$ and $\mathbf{3c}^-/\mathbf{3c}^{2-}$ given in Table 2. The values of K_C in acetonitrile ($K_C(CH_3CN,298\ K) = 7.9 \times 10^{12}$, $\Delta E_{1/2} = 0.76$ V) and in tetrahydrofuran ($K_C(THF,298\ K) = 6.2 \times 10^{15}$, $\Delta E_{1/2} = 0.93$ V) are typical of a radical anion of the class III in which the "single" electron is delocalized between the two manganese centers over the bridging diaza heterocycle.[43]

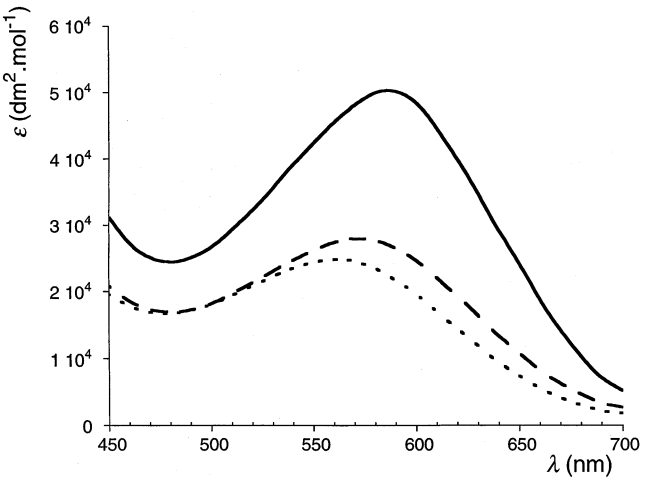

Figure 10. Solvatochromism of complex **3c** in the region 450−700 nm characterized by the variation of the extinction coefficient ϵ (dm^2 mol^{-1}) and the value of λ_{max} (nm) with the polarity of the solvent: (−) in hexane (9.8×10^{-5} M, λ_{max} 586 nm, $\epsilon_{586} = 5.0 \times 10^4$); (- - -), in dichloromethane (9.8×10^{-5} M, λ_{max} 569 nm, $\epsilon_{569} = 2.8 \times 10^4$); (···) in acetonitrile (9.4×10^{-5} M, λ_{max} 561 nm, $\epsilon_{561} = 2.5 \times 10^4$).

Complex **3c** is a blue compound which displays a net negative solvatochromism[44] associated with the relatively intense metal-to-ligand charge-transfer transition (MLCT) band located at ca. 590 nm, as illustrated in Figure 10. Negative solvatochromism understands that more polar solvents stabilize more the ground state than the excited state, thus leading to a decrease of both the wavelength and the extinction coefficient of the corresponding transition.[45] However, solvatochromism of a binuclear nonpolar complex such as **3c** questions the nature of both the ground and the Franck−Condon excited states.[46]

A similar system has been studied by Kaim and coworkers: the binuclear dark blue and air-sensitive complexes of the formula $(CpR)(CO)_2Mn(pyrazine)Mn(CO)_2(CpR)$.[47] The latter revealed some similarities in their spectrochemical properties with Ru(II) analogues. The authors reported only one reversible reduction wave at around −1.38 V vs SCE that is at potentials more negative than those reported herein for **3c** but close to those reported for uncoordinated pyrazine[38a] (−1.40 V in DMF with a glassy-carbon working electrode). Worthy of note, the authors did not report any other reduction wave at a more negative potential.

Chemical reduction of a solution of **3c** in THF by reaction with a potassium mirror revealed a spectral

(41) (a) Michaelis, L. *Biochem. Z.* **1932**, *250*, 564. (b) Michaelis, L.; Hill, E. S. *J. Am. Chem. Soc.* **1933**, *55*, 1491. (c) Michaelis, L. *J. Prakt. Chem.* **1959**, *9*, 164.

(42) (a) Rieke, R. D.; Arney, J. S.; Rich, W. E.; Willeford, B. R.; Poliner, B. S. *J. Am. Chem. Soc.* **1975**, *97*, 5951. (b) Rieke, R. D.; Henry, W. P.; Arney, J. S. *Inorg. Chem.* **1987**, *26*, 420.

(43) (a) Richardson, D. E.; Taube, H. *Inorg. Chem.* **1981**, *20*, 1278. (b) Richardson, D. E.; Taube, H. *Coord. Chem. Rev.* **1984**, *60*, 107. (c) Ward, M. D. *Chem. Soc. Rev.* **1995**, 121. (d) Kaim, W.; Klein, A.; Glöckle, M. *Acc. Chem. Res.* **2000**, *33*, 755. (e) Demadis, K. D.; Hartshorn, C. M.; Meyer, T. J. *Chem. Rev.* **2001**, *101*, 2655. (f) Lambert, C.; Nöll, G. *J. Am. Chem. Soc.* **1999**, *121*, 8434. (g) Bonvoisin, J.; Launay, J. P.; Rovira, C.; Veciana, J. *Angew. Chem.* **1994**, 106, 2190; *Angew. Chem., Int. Ed. Engl.* **1994**, *33*, 2106.

(44) (a) Drago, R. S. *J. Chem. Soc., Perkin Trans. 2* **1992**, 1827. (b) Drago, R. S. *J. Org. Chem.* **1992**, *57*, 6547. (c) Drago, R. S.; Hirsh, M. S.; Ferris, D. C.; Chronister, C. W. *J. Chem. Soc., Perkin Trans. 2* **1994**, 219. (d) Marcus, Y. *Chem. Soc. Rev.* **1993**, *22*, 409. (e) Thomas, J. A.; Hutchings, M. G.; Jones, C. J.; McCleverty, J. A. *Inorg. Chem.* **1996**, *35*, 289.

(45) *Developments in the Chemistry and Technology of Organic Dyes*; Griffiths, J., Ed.; Blackwell Scientific: Oxford, U.K., 1983.

(46) Dodsworth, E. S.; Lever, A. B. P. *Coord. Chem. Rev.* **1990**, *97*, 271.

(47) Gross, R.; Kaim, W. *Inorg. Chem.* **1986**, *25*, 498.

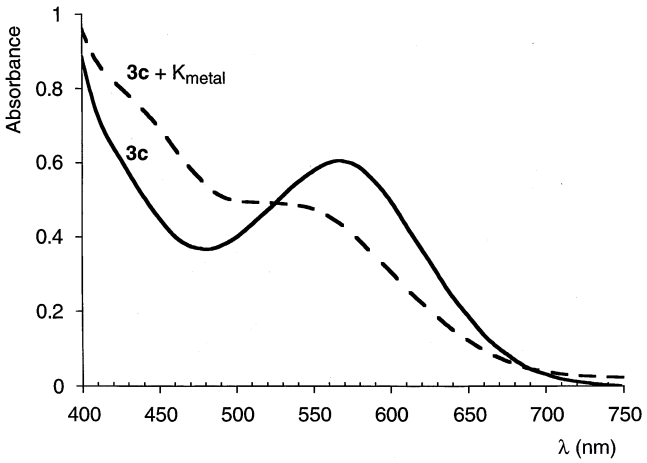

Figure 11. Spectral changes of a THF solution of complex **3c** ($c \approx 2.75 \times 10^4$ M, $\epsilon_{568} \approx 4 \times 10^4$) upon reduction over a potassium mirror (absorption vs wavelength in nm): continuous curve, solution of **3c** in THF; dashed curve, spectrum after reaction with K. Main changes in the absorption spectrum occur in the 400−750 nm region.

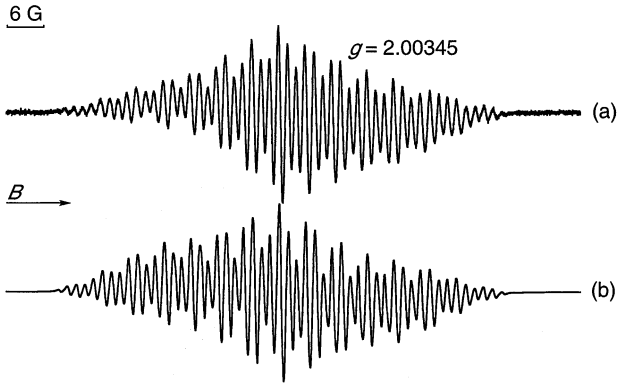

Figure 12. Measured (a) and simulated (b) X-band ESR spectra of the radical anion **3c**$^-$ ($c \approx 1.1 \times 10^{-3}$ M, g = 2.003 45) in THF at 293 K, formed by reaction of **3c** with potassium metal: microwave power, 2 mW; modulation frequency, 100 kHz; modulation amplitude, 0.5 G; sweep time, 83.9 s.

dependence of the solute over its oxidation state in solution. This reduction reaction induced relevant changes in the 400−750 nm region of the visible absorption spectrum in THF (Figure 11) and clearly obliterated the MLCT transition of **3c** observed at 570 nm in THF.

An X-band ESR analysis of a solution containing reduced **3c** indicated the presence of a paramagnetic species, putatively **3c**$^-$, having a half-life time of ca. 30 min, at 298 K, under an argon atmosphere. A value of 2.003 45 was determined for the g factor (Figure 12a). Unfortunately, all our attempts at acquiring ENDOR spectra and therefore at gaining a better estimation of the a^{CH} hyperfine coupling constants failed so far. However, the hyperfine structures were thoroughly analyzed from the ESR spectrum (Figure 12a), satisfactorily simulated,[48] and refined (Figure 12b). The following hyperfine coupling constants were extracted, considering that spin density was very probably essentially located mostly at the quinoxaline nucleus and, to a lesser extent, at the two metal centers: $a(^{55}\text{Mn}, I = {}^5/_2) = 4.6$ G, $a(^{14}\text{N}, I = {}^3/_2) = 6.1$ G, a(H,C−H) = 1.3 G, a(H,CH) = 1.6 G. In the pyrazine-based system investigated by Kaim and Gross, the values of g for three Mn(I) complexes, whose differences are ascribed to different degrees of substitution at the Cp fragment, are lower than that of the free electron ($g_e = 2.002\ 32$).[49]

McConnell's postulate defines a linear relationship between hyperfine coupling constants and the π-spin population in aromatic radical ions. A comparison of the hyperfine coupling constants a(H) and $a(^{14}\text{N})$ assigned to the radical anion **3c**$^-$ with the values reported by Bock and co-workers for the radical anion of 2,3-diphenylquinoxaline ($a(\text{H}_{5,8}) = 2.39$ G, $a(\text{H}_{6,7}) = 1.40$ G, $a(^{14}\text{N}) = 5.25$ G) clearly suggests a lower π-spin density at the benzo fragment of the quinoxaline nucleus of **3c** and a significant transfer of spin density to the two nitrogen atoms and the two manganese centers. A similar fact has been pointed out for the pyrazine-based dinuclear Mn(I) complexes by Kaim and Gross, who furthermore underscored the absence of spin density at the surrounding Cp ligands. With the radical anion **3c**$^-$, we seemingly have a similar situation where spin density is negligible both at the two phenylene fragments and at the two endo-phenyl groups overlapping the heterocycle. This is not exceptional, as the π-system presents discontinuities at the benzylic positions and at the junction of the heterocycle with the two twisted phenylene groups. Therefore, like **3c**, the dinuclear radical anion **3c**$^-$ is homovalent.

Conclusion

In this article we report on new C−C bond-forming reactions between a series of cyclometalated aromatic ligands and the two symmetrically substituted diazoalkanes Ar_2CN_2. These reactions are promoted by heat, which enables the partial decarbonylation of the *cis*-(LC)Mn(CO)$_4$ substrate, thus creating a vacant coordination site. The formation of a metal−alkylidene intermediate is followed by a series of molecular rearrangements that lead in one case ($Ar_2CN_2 = (C_6H_5)_2CN_2$) to stable chelated ($\eta^3$-trihaptobenzyl)Mn(CO)$_3$ complexes and in the other case ($Ar_2CN_2 = C_{12}H_8CN_2$) to a new class of stable mono- and dinuclear appended (η^5-fluorenyl)Mn(CO)$_3$ complexes. In most cases these reactions are efficient and the conversions are higher than 50%. These new coupling reactions might show some interesting applications, especially for the synthesis of organometallic C−C bond-based polymers. For this latter purpose, bis-diazoalkanes and poly-cyclometalated aromatics are the substrates of choice. Of course, we have shown here only the results pertaining to the use of two symmetrically substituted diaryldiazoalkanes. We are currently addressing the stereoselectivity issues raised by the use of unsymmetrically substituted diazoalkanes and further investigate the synthetic applications of our new method of preparation of substituted CpM(CO)$_3$-type complexes described herein. Electrochemical studies of various mono- and dinuclear spiralenes demonstrate that reduction processes are

(48) Winsim program from the Public EPR Software Tools distribution (National Institute of Environmental Health Sciences, http://EPR.niehs.nih.gov): Duling, D. R. *J. Magn. Reson., Ser. B* **1994**, *104*, 105.

(49) (a) Weil, J. A.; Bolton, J. R.; Wertz, J. E. In *Electron Paramagnetic Resonance, Elementary Theory and Practical Applications*; Wiley: New York, 1994. (b) Kaim, W. *Inorg. Chem.* **1984**, *23*, 3365. (c) Gerson, F. In *Hochauflösende ESR−Spektroskopie, dargestellt anhand aromatischer Radikal-Ionen*; Först, W., Grünewald, H., Eds.; Verlag Chemie: Weinheim, Germany, 1967.

mostly ligand-based and involve the reversible transfer of one electron. With complex **3c**, the scaffolds constisting of coordinated $Mn(CO)_3$ fragments prevent the aromatic groups surrounding the central heterocycle from coupling.

The electron-accepting character of these helical complexes motivates further studies of their application in the building of electroactive materials, whereby conduction is based on charge transport mechanisms such as those suspected for DNA, i.e. charge "hopping".[50] Spiralenes consist of intramolecular stacks of covalently linked nonconjugated aromatic rings, for which electronic properties (Lewis-type acceptors or donors) can be varied by the judicious choice of substituents at both precursor substrates: in the future, this property could be used for the synthesis of spiralene-type prototypes of molecular charge-transfer complexes, by the reaction of $(LC)Mn(CO)_4$ complexes containing an electron-accepting pyrazine or quinoxaline nucleus, such as in **3b,** with diazoalkanes bearing a strong electron donor aromatic such as tetrathiafulvalenyl or benzotetrathiafulvalenyl. Further studies are now underway to evaluate such applications.

Experimental Section

General Considerations. All experiments were carried out under a dry atmosphere of argon with dry and degassed solvents. Starting (η^6-arene)tricarbonylchromium complexes were synthesized according to published procedures.[3,6d] NMR spectra were acquired on Bruker DRX 500 (^{13}C and ^1H nuclei) and AC 300 (^1H nucleus) spectrometers at room temperature unless otherwise stated. Chemical shifts are reported in parts per million downfield of Me_4Si. X-Band ESR spectra (9.376 11 GHz) were recorded at room temperature with a Bruker ESP 300 spectrometer using a 3 mm inner-diameter sample tube loaded under argon with a freshly prepared analyte. IR spectra were measured with a Perkin-Elmer FT spectrometer. Mass spectra were recorded at the Service of Mass Spectrometry of the University Louis Pasteur (FAB+) and at the Analytical Center of the Chemical Institute of the University of Bonn (EI). Elemental analyses (reported in percent mass) were performed at the Service d'Analyses of the "Institut de Chimie de Strasbourg" and at the analytical center of the "Institut Charles Sadron" in Strasbourg.

Electrochemical Experiments. All electrochemical experiments were carried out at room temperature (25 °C) under an atmosphere of argon with a Princeton Applied Research 273 potentiostat (Model 270/250) computer-controlled with a EGCS Research Electrochemistry software version 4.23. Tetra-*n*-butylammonium hexafluorophosphate was used as supporting electrolyte in 0.1 M solutions of dry and deaerated solvents. Solid $n\text{-}Bu_4N^+PF_6^-$ was dried under vacuum for 2 days at 70 °C prior to use in electrochemical experiments. Cyclic voltammetry experiments were carried out under an atmosphere of Ar using an undivided cell comprising a ca. 2 mm diameter Pt-bead working electrode, a 1 mm diameter Pt wire as counter electrode, and a ca. 1 mm diameter Ag wire as the pseudo-reference electrode. Unless otherwise stated, measures were referenced against the ferrocene−ferrocenium (Fc^+/Fc) couple. Values of potentials were extrapolated against the SCE. Coulometric experiments were carried out using a cell consisting of a spiral-shaped Pt wire as cathode, a straight Pt wire as anode, and a KCl-saturated calomel reference electrode. The last two were separated from the solution containing the analyte by a bridge consisting of a fritted-glass tube containing a 0.1 M solution of supporting electrolyte. Cathodic reductions were carried out at a potential ca. 200 mV lower than the $E_{1/2}$ potential of the studied redox couple.

Experimental Procedure for the X-ray Diffraction Analysis of Compounds 1b,c, 2b, 3c−e, and 5a,c. Acquisition and processing parameters are displayed in Table 1. Reflections were collected with a Nonius KappaCCD diffractometer using Mo Kα graphite-monochromated radiation (λ = 0.710 73 Å). The structures of **5a** and **5c** were refined on F^2: the programs used for structure solution and refinement were SHELXS97 and SHELXL-97.[51] For both compounds **5a** and **5c** an empirical absorption correction was applied (minimum/maximum transmission 0.3227/0.4063 (**5a**) and 0.5026/0.6296 (**5c**)). The other structures were solved using direct methods and were refined against $|F|$, and for all pertaining computations the Nonius OpenMoleN package was used.[52] Hydrogen atoms were introduced as fixed contributors. The absolute structure of **3e** was determined by refining Flack's x parameter ($x = 0.03$).

General Procedure for Reactions of Cyclometalated Substrates with Diaryldiazomethanes. The complex was dissolved in either pure *n*-heptane or toluene (or a mixture of both). The resulting solution was brought to reflux, and a solution of diaryldiazomethane in toluene was added dropwise via a syringe. The reaction mixture was further stirred, the solution was cooled to room temperature, and the solvents were evaporated under reduced pressure. The crude residue was dissolved in CH_2Cl_2, and SiO_2 was added to the resulting solution. The solvent was removed under reduced pressure and the coated silica gel loaded on the top of a chromatographic column packed in hexane at subambient temperature for further separation of the main product from organic byproducts.

Preparation of 2-[Tricarbonyl{η^6-2′-[tricarbonyl(η^5-fluoren-9-yl)manganese(I)]phenyl}chromium(0)]-pyridine (1c). Conditions and reagents for this reaction are as follows: complex **1a** (200 mg, 0.43 mmol), heptane (10 mL), toluene (10 mL), ebullition; 9-diazofluorene (168 mg, 0.87 mmol) in toluene (5 mL), dropwise addition over 30 min via a syringe; further stirring for 1 h. The crude residue was dissolved in CH_2Cl_2, and SiO_2 was added to the resulting solution. Chromatography on SiO_2 at 10 °C: **1c** (1:1 CH_2Cl_2/acetone), recrystallization (CH_2Cl_2/hexane), air-stable bright yellow-orange crystals (140 mg, 54% yield). Anal. Calcd for $C_{24}H_{16}NO_6CrMn$: C, 60.74; H, 2.36; N, 2.72. Found: C, 60.40; H, 2.29; N, 2.76. IR (CH_2Cl_2): ν(CO) 2021 (m), 1969 (s), 1936 (m), 1897 (m) cm^{-1}. ^1H NMR ($CDCl_3$): δ 8.36 (d, 1H, ^3J = 3.2 Hz), 8.14 (t, 2H, ^3J = 7.5 Hz), 7.97 (d, 1H, ^3J = 8.5 Hz), 7.50 (t, 1H, ^3J = 7.7 Hz), 7.30 (t, 1H, ^3J = 7.6 Hz), 7.10 (t, 1H, ^3J = 7.3 Hz), 6.92−6.85 (m, 4H), 6.54 (d, 1H, ^3J = 7.3 Hz), 6.47 (d, 1H, ^3J = 6.3 Hz, H_{ArCr}), 6.07 (d, 1H, ^3J = 6.1 Hz, H_{ArCr}), 5.87 (t, 1H, ^3J = 6.1 Hz, H_{ArCr}), 5.66 (t, 1H, ^3J = 6.2 Hz, H_{ArCr}). ^{13}C NMR ($CDCl_3$): δ 232.7, 224.3, 153.9, 148.9, 135.0, 128.6, 127.2, 125.4, 125.3, 124.9, 124.7, 123.9 (2C), 123.6, 123.0, 112.2, 107.3, 106.3, 102.7, 101.4, 95.1, 94.8, 92.4, 91.5, 90.7, 78.0.

Synthesis of Tetracarbonyl[3-methyl-2-(phenyl-$\kappa C^{2'}$)-pyridine-κN]manganese(I) (2a). A solution of $(PhCH_2)Mn(CO)_5$ (5.64 g, 19.7 mmol) and 3-methyl-2-phenylpyridine (4.0 g, 23.6 mmol) in dry and degassed heptane (25 mL) was brought to reflux and stirred for 24 h. The resulting mixture was cooled to room temperature and the solvent evaporated under reduced pressure. The crude oily mixture was redis-

(50) (a) Grinstaff, M. W. *Angew. Chem., Int. Ed.* **1999**, *38*, 3629; *Angew. Chem.* **1999**, *111*, 3845. (b) Ly, D.; Sanii, L.; Schuster, G. B. *J. Am. Chem. Soc.* **1999**, *121*, 9400. (c) Giese, B. *Acc. Chem. Res.* **2000**, *33*, 631. (d) Giese, B.; Spichty, M. *Chem. Phys. Chem.* **2000**, *1*, 195. (e) Grozema, F. C.; Berlin, Yu. A.; Siebbeles, L. D. A. *J. Am. Chem. Soc.* **2000**, *122*, 10903. (f) Berlin, Yu. A.; Burin, A. L.; Ratner, M. A. *J. Am. Chem. Soc.* **2001**, *123*, 260. (g) Bixon, M.; Jortner, J. *J. Am. Chem. Soc.* **2001**, *123*, 12556. (h) Cai, Z.; Gu, Z.; Sevilla, M. D. *J. Phys. Chem. B* **2000**, *104*, 10406.

(51) (a) SHELXS97: Sheldrick, G. M. *Acta Crystallogr.. Sect. A* **1990**, *46*, 467. (b) Sheldrick, G. M. SHELXL-97; University of Göttingen, Göttingen, Germany, 1997.

(52) Fair, C. K. In *MolEN: An Interactive Intelligent System for Crystal Structure Analysis*; Nonius: Delft, The Netherlands, 1990.

solved in CH_2Cl_2 and silica gel added to the resulting solution. The solvent was removed under reduced pressure and the coated SiO_2 loaded on the top of a silica gel column packed in dry deaerated hexane. A yellow band containing **2a** was eluted with a 7:3 CH_2Cl_2/hexane mixture. Evaporation of the solvents afforded compound **2a** as a pure yellow solid (3.74 g, 50% yield). Anal. Calcd for $C_{16}H_{10}NO_4Mn$: C, 57.33; H, 3.01; N, 4.18. Found: C, 57.43; H, 3.05; N, 4.14. IR (CH_2Cl_2): ν(CO) 2074 (m), 1989 (s), 1974 (s), 1929 (s) cm^{-1}. ^1H NMR ($CDCl_3$, 400 MHz): δ 8.77 (d, 1H, ^3J = 5.4 Hz), 8.06 (m, 2H), 7.63 (d, 1H, ^3J = 7.6 Hz), 7.28 (t, 1H, ^3J = 7.5 Hz), 7.22 (d, 1H, ^3J = 7.6 Hz), 7.03 (t, 1H, ^3J = 6.6 Hz), 2.80 (s, 3H). ^{13}C NMR ($CDCl_3$, 100 MHz): δ 220.2 (CO), 214.2 (2CO), 213.9 (CO), 176.2, 164.8, 152.1, 148.5, 142.2, 141.7, 132.6, 129.2, 128.5, 123.6, 121.5, 24.0.

Preparation of Tricarbonyl{3-methyl-2-[1′,2′,7′-η:2-(diphenylmethylene)phenyl]pyridine-κN}manganese-(I) (2b). Conditions and reagents for this reaction are as follows: complex **2a** (400 mg, 1.43 mmol), *n*-heptane (10 mL), ebullition; diazodiphenylmethane (1.18 g, 5.71 mmol), toluene (5 mL), dropwise addition over 30 min; further stirring under reflux for 1 h. Chromatography with a SiO_2 column packed in dry hexane at 5 °C: **2b** (CH_2Cl_2), recrystallization from ether and hexane, orange powder (376 mg, 63% yield). Anal. Calcd for $C_{28}H_{20}NO_3Mn$: C, 71.04; H, 4.26; N, 2.96. Found: C, 70.92; H, 4.32; N, 2.64. IR (CH_2Cl_2): ν(CO) 2000 (m), 1913 (s), 1901 (s) cm^{-1}. ^1H NMR ($CDCl_3$, 500 MHz): δ 7.76 (d, 2H, ^3J = 9.1 Hz, $H_{o-Ph,exo}$), 7.60 (d + t, 2H, $H_{\alpha-Py}$ + $H_{m-phenylene}$), 7.47 (d, 1H, ^3J = 9.8 Hz, $H_{o-Ph,endo}$), 7.34 (m, 5H, $2H_{m-Ph,exo}$ + $2H_{o-phenylene}$ + $H_{m-phenylene}$), 7.21 (t, 1H, ^3J = 9.2 Hz, $H_{p-Ph-exo}$), 7.12 (d, 1H, ^3J = 9.8 Hz, $H_{\gamma-Py}$), 6.84 (t, 1H, ^3J = 9.5 Hz, $H_{m-Ph,endo}$), 6.59 (m, 2H, $H_{p-Ph,endo}$ + $H_{\beta-Py}$), 6.48 (t, 1H, ^3J = 9.3 Hz, $H_{m-Ph,endo}$), 6.18 (d, 1H, ^3J = 8.7 Hz, $H_{o-Ph,endo}$), 2.18 (s, 3H, Me). ^{13}C NMR ($CDCl_3$): δ 231.7 (CO), 221.4 (CO), 220.8 (CO), 156.8, 148.9, 148.2, 147.8, 138.7, 136.3, 134.5, 133.2, 132.1, 130.9, 129.9, 128.5, 128.1, 126.0, 125.8, 125.7, 125.4, 123.9, 123.8, 114.3, 97.3, 77.7, 17.0.

Preparation of 3-Methyl-2-{2′-[tricarbonyl(η^5-fluoren-9-yl)manganese(I)]phenyl}pyridine (2c). Conditions and reagents for this reaction are as follows: complex **2a** (400 mg, 1.24 mmol), toluene (10 mL), ebullition; 9-diazofluorene (549 mg, 2.86 mmol), toluene (5 mL), dropwise addition over 45 min; further stirring under reflux of toluene for 45 min. Chromatography with a SiO_2 column packed in dry hexane and cooled at 5 °C: **2c** (7:3 hexane/acetone), bright canary yellow powder (367 mg, 71% yield). Anal. Calcd for $C_{28}H_{18}NMnO_3$: C, 71.34; H, 3.85; N, 2.97. Found: C, 71.39; H, 3.96; N, 2.84. IR (CH_2Cl_2): ν(CO) 2076 (m), 1933 (s) cm^{-1}. ^1H NMR ($CDCl_3$): δ 8.32 (d, 1H, ^3J = 7.8 Hz), 8.12 (d, 1H, ^3J = 4.2 Hz), 7.96 (d, 2H, ^3J = 8.3 Hz), 7.70 (t, 1H, ^3J = 7.1 Hz), 7.60 (t, 1H, ^3J = 7.4 Hz), 7.52 (d, 1H, ^3J = 7.1 Hz), 7.31 (d, 1H, ^3J = 8.3 Hz), 7.08 (m, 4H), 6.96 (d, 1H, ^3J = 7.6 Hz), 6.75 (m, 1H), 1.57 (s, 3H). ^{13}C NMR ($CDCl_3$, 100 MHz, 263 K): δ 225.2 (3CO), 157.9, 146.4, 141.9, 137.3, 135.3, 131.4, 131.1, 130.5, 128.8, 128.5, 127.8, 126.3, 125.5 (2C), 124.8, 124.4, 123.5, 123.1, 121.8, 107.5, 105.5, 94.5, 91.0, 83.9, 19.1.

Preparation of [2,3-(Diphenyl-$\kappa C^{2'}$,$\kappa C^{2''}$]quinoxaline-κN^1,κN^2)bis(tetracarbonylmanganese(I)) (3b). A solution of **3a** (2 g, 7 mmol) and $(PhCH_2)Mn(CO)_5$ (4 g, 14 mmol) in heptane (30 mL) was brought to reflux and stirred for 20 h. The resulting deep purple-red solution was then cooled to room temperature and the solvent evaporated under reduced pressure. The crude solid mixture was dissolved in CH_2Cl_2, silica gel was added, and the solvent was evacuated under reduced pressure. The resulting coated silica gel was loaded on the top of a SiO_2 column packed in dry hexane. A deep purple band containing compound **3a** was eluted with a 1:1 CH_2Cl_2/hexane mixture. Removal of the solvents under reduced pressure afforded a purple powder (3 g, 63% yield) that was recrystallized from a mixture of CH_2Cl_2 and hexane. Anal. Calcd for $C_{28}H_{12}N_2O_8Mn_2$: C, 54.75; H, 1.97; N, 4.56. Found: C, 54.87; H, 1.79; N, 4.53. IR (CH_2Cl_2): ν(CO) 2076 (m), 1999 (s), 1981 (s), 1941 (s). ^1H NMR ($CDCl_3$): δ 8.59 (m, 2H), 8.19 (d, 2H, ^3J = 7.3 Hz), 7.99 (d, 2H, ^3J = 8.0 Hz), 7.80 (m, 2H), 7.28 (t, 2H, ^3J = 7.3 Hz), 7.01 (t, 2H, ^3J = 8.1 Hz). ^{13}C NMR ($CDCl_3$, 263 K): δ 220.6 (CO), 213.9 (CO), 212.7 (CO), 181.1, 161.9, 149.3, 141.5, 131.6, 130.9, 130.6, 127.6, 123.6, 115.1.

Synthesis of *lk*-{2,3-Di[1′2′7′:η-2′-(diphenylmethylene)-phenyl]quinoxaline-κN^1,κN^2}bis(tricarbonylmanganese-(I)) (3c). A solution of diphenyldiazomethane (784 mg, 4 mmol) in toluene (5 mL) was added to a boiling solution of **3b** (411 mg, 0.67 mmol) in a 1:4 heptane/toluene mixture within 10 min. The color of the medium quickly changed from deep purple to dark blue. The solution was further stirred for 30 min and subsequently cooled to room temperature. The solvents were evaporated under reduced pressure, and the crude residue was dissolved in CH_2Cl_2. Silica gel was added to the resulting dark solution and the solvent evaporated subsequently. The coated silica gel was loaded on the top of a SiO_2 column packed in hexane. The main blue band containing **3c** was eluted with pure CH_2Cl_2. Evaporation of the solvent afforded compound **3c** as a dark blue powder (358 mg, 60% yield) soluble in almost any organic solvent. Crystals suitable for X-ray diffraction analysis were obtained at +4 °C by the slow evaporation of a solution of **3c** in pure *n*-heptane. Anal. Calcd for $C_{52}H_{32}N_2O_6Mn_2$: C, 70.12; H, 3.65; N, 3.15. Found: C, 70.17; H, 3.65; N, 3.04. High-resolution MS (FAB+): calcd for $C_{52}H_{32}N_2O_6Mn_2$ 890.102 13, found 890.101 33. IR (CH_2Cl_2): ν(CO) 2000 (m), 1931 (s), 1907 (s) cm^{-1}. UV−visible (hexane; λ_{max}, nm (ϵ, $dm^2\ mol^{-1}$)): 351 (1.17×10^5), 586 (5.0×10^4). UV−visible (CH_2Cl_2; λ_{max}, nm (ϵ, $dm^2\ mol^{-1}$)): 347 (7.4×10^4), 569 (2.8×10^4). UV−visible (CH_3CN; λ_{max}, nm (ϵ, $dm^2\ mol^{-1}$)): 344 (6.8×10^4), 561 (2.5×10^4) nm. ^1H NMR ($CDCl_3$, 273 K): δ 7.87 (broad d, 4H, $H_{o-Ph,exo}$), 7.60 (m, 2H, $H_{quinoxaline}$), 7.54 (m, 2H, $H_{quinoxaline}$), 7.39 (broad m, 6H, $H_{m-Ph,exo}$+$H_{m-phenylene}$), 7.27 (broad m, 4H, $H_{p-Ph,exo}$ + $H_{o-Ph,endo}$), 7.18 (broad m, 4H, $H_{m-phenylene}$ + $H_{o-phenylene}$), 7.09 (d, 2H, ^3J = 8.8 Hz, $H_{o-phenylene}$), 6.90 (t, 2H, ^3J = 7.2 Hz, $H_{m-Ph,endo}$), 6.65 (d, 2H, ^3J = 7.2 Hz, $H_{o-Ph,endo}$), 6.39 (t, 2H, ^3J = 6.9 Hz, $H_{p-Ph,endo}$), 6.30 (t, 2H, ^3J = 7.4 Hz, $H_{m-Ph,endo}$). ^1H NMR (C_6D_6, 293 K): δ 7.87 (d, 4H), 7.54 (m, 4H), 7.49 (d, 2H), 7.23 (t, 4H), 7.16 (m, 2H), 7.06 (t, 4H), 6.83 (t, 2H), 6.66 (t, 4H), 6.60 (m, 2H), 6.35 (t, 2H), 6.13 (t, 2H). ^{13}C NMR ($CDCl_3$, 273K): δ 230.3 (CO), 220.9 (CO), 219.8 (CO), 146.2, 146.1, 139.4, 134.9, 133.4, 133.2, 131.9, 131.6, 131.4, 128.7, 127.6, 126.3, 125.4, 124.9, 124.6, 124.1, 115.6, 86.9, 76.2. MS (FAB^+): *m*/Hz 890 $[M]^+$, 806 $[M - 3CO]^+$, 778 $[M - 4CO]^+$, 722 $[M - 6CO]^+$.

Synthesis of 2,3-Di{2′-[tricarbonyl(η^5-fluoren-9-yl)-manganese(I)]phenyl}quinoxaline (3d). A solution of 9-diazofluorene (500 mg, 2.6 mmol) in toluene (5 mL) was added to a boiling solution of **3b** (500 mg, 0.81 mmol) in toluene over 30 min. The color of the medium progressively changed from deep purple to orange-yellow. The solution was further stirred for 30 min and subsequently cooled to room temperature. The solvent was evaporated under reduced pressure and the crude residue dissolved in CH_2Cl_2. Silica gel was added to the resulting solution and the solvent evaporated under reduced pressure. The coated silica gel was loaded on the top of a SiO_2 column packed in hexane. The first orange fraction was eluted with a 1:4 CH_2Cl_2/hexane mixture and assigned to unreacted amounts of 9-diazofluorene. A yellow band containing **3d** was eluted with a 7:3 CH_2Cl_2/hexane mixture. Evaporation of the solvent afforded compound **3d** as a canary yellow powder (570 mg, 79% yield). Crystals suitable for X-ray diffraction analysis were obtained at −20 °C by the diffusion method in a narrow glass tube containing a concentrated CH_2Cl_2 solution of **3d** (lower layer) and pure heptane (upper layer). Anal. Calcd for $C_{52}H_{28}N_2O_6Mn_2$: C, 70.44; H, 3.18; N, 3.16. Found: C, 70.60; H, 3.25; N, 3.21. High-resolution MS (FAB+): calcd for $C_{52}H_{29}N_2O_6Mn_2$ (MH^+) 887.078 655, found 887.078 307. IR (CH_2Cl_2): ν(CO) 2015 (m), 1937 (s) cm^{-1}. ^1H NMR (C_6D_6): δ 8.01 (d, 2H), 7.90 (m, 2H, $H_{quinoxaline}$), 7.61 (d, 2H), 7.49 (d, 2H), 7.25 (m, 2H, $H_{quinoxaline}$), 7.09 (d, 2H), 6.86−6.72 (m, 6H), 6.43

(t, 2H), 6.35 (d, 2H), 6.25 (t, 2H), 6.19 (d, 2H), 5.75 (t, 2H). ^{1}H NMR ($CDCl_3$, 283 K): δ 8.13 (d, 2H, ^3J = 7.5 Hz, $H_{phenylene}$), 8.00 (d, 2H, ^3J = 8.6 Hz, $H_{fluorenyl}$), 7.96 (m, 2H, $H_{quinoxaline}$), 7.79 (d, 2H, ^3J = 7.3 Hz, $H_{fluorenyl}$), 7.74 (m, 2H, $H_{quinoxaline}$), 7.25−7.19 (m, 4H, $H_{phenylene}$), 7.10 (d, 2H, ^3J = 7.8 Hz, $H_{phenylene}$), 7.06 (t, 2H, ^3J = 7.5 Hz, $H_{fluorenyl}$), 6.93 (dd, 2H, ^3J = 6.6 Hz, ^3J = 8.2 Hz, $H_{fluorenyl}$), 6.43 (t, 2H, ^3J = 7.5, $H_{fluorenyl}$), 6.14 (d, 2H, ^3J = 8.9 Hz, $H_{fluorenyl}$), 6.05 (dd, 2H, ^3J = 6.6 Hz, ^3J = 8.4 Hz, $H_{fluorenyl}$), 5.86 (d, 2H, ^3J = 7.8 Hz, $H_{fluorenyl}$). ^{13}C NMR ($CDCl_3$, 283 K): δ 224.9 (3CO), 153.7, 141.1, 138.0, 133.6, 132.6, 130.3, 129.9, 129.5, 128.6, 128.5, 126.7, 125.7, 125.3, 125.1, 124.6, 124.0, 123.4, 122.5, 108.1, 102.5, 96.6, 90.5, 83.3. MS (FAB+): *m*/Hz 887 $[MH]^+$, 802 $[M - 3CO]^+$, 746 $[MH - 5CO]^+$, 718 $[M - 6CO]^+$, 663 $[M - 6CO - Mn]^+$, 608 $[M - 6CO - 2Mn]^+$.

Preparation of Poly([2,3-di{2′-[tricarbonyl(η^5-fluoren-9-yl)manganese(I)]phenyl}quinoxaline)silver(I)]tetrafluoroborate) (3e). A stoichiometric mixture of complex **3d** and $AgBF_4$ in dry acetone was boiled for 10 min until the color changed from yellow to red. The solution was then filtered through Celite and the solvent evaporated. The crude mixture was then recrystallized from a mixture of MeOH, CH_2Cl_2, and hexane and the red microcrystalline powder washed thrice with 20 mL of dry *n*-hexane. Crystals suitable for X-ray diffraction analysis were obtained by the slow diffusion at −20 °C of a concentrated solution of the former red crystals in a 1:1 MeOH/tetrahydrofuran mixture (lower layer) into an upper layer of dry heptane. Anal. Calcd for $C_{52}H_{28}Mn_2N_2O_6AgBF_4 \cdot CH_2Cl_2 \cdot CH_3OH$: C, 54.13; H, 2.86; N, 2.34. Found: C, 54.11, H, 2.70; N, 2.34.

Synthesis of 2-{2′-[Tricarbonyl(η^5-fluoren-9-yl)manganese(I)]phenyl}azabenzo-6,6-dimethylbicyclo[3.1.1]-heptane (4b). Conditions and reagents for this reaction are as follows: complex **4a** (230 mg, 0.55 mmol), *n*-hexane/toluene (10:1, 11 mL), ebullition; 9-diazofluorene (212 mg, 1.10 mmol), toluene (2.5 mL), dropwise addition over 30 min; further stirring for 3 h. Flash chromatography on SiO_2 at 6 °C: **4b** (*n*-hexane/acetone, 1:1), light yellow-orange powder (260 mg, 0.47 mmol, 85% yield). $[\alpha]_D(CH_2Cl_2, 20\ °C) = -33 \pm 1°\ dm^{-1}\ g^{-1}$ mL (c = 3.05 mM). Anal. Calcd for $C_{34}H_{26}NO_3Mn$: C, 74.04; H, 4.75; N, 2.54. Found: C, 73.88; H, 4.90; N, 2.34. High-resolution MS (FAB$^+$): calcd for $C_{34}H_{27}NO_3Mn$ (MH^+) 552.137 168, found 552.137 140 amu. IR (CH_2Cl_2): ν(CO) 2014, 1931 cm^{-1}. ^{1}H NMR ($CDCl_3$, 20 °C, 500 MHz): δ 8.30 (d, 1H, ^3J = 7.1 Hz), 7.98 (d, 2H, ^3J = 8.7 Hz), 7.71 (d, 1H, ^3J = 7.6 Hz), 7.66 (m, 1H), 7.59 (t, 1H, ^3J = 7.5 Hz), 7.29 (m, 1H), 7.24 (d, 1H, ^3J = 8.7 Hz), 7.12 (m, 3H), 7.03 (t, 1H, ^3J = 7.4 Hz), 6.61 (d, 1H, ^3J = 7.5 Hz), 6.43 (d, 1H, ^3J = 7.7 Hz), 2.50 (m, 3H), 2.13 (m, 1H), 1.25 (m, 4H), 0.88 (m, 1H), 0.20 (s, 3H). ^{13}C NMR ($CDCl_3$, 125 MHz): δ 225.4 (CO), 155.9, 155.6, 143.1, 139.5, 136.0, 132.3, 130.6, 129.9, 128.8 (2C), 127.6, 127.4, 124.9, 124.6, 124.4 (2C), 124.2, 123.8, 120.1, 108.0, 107.5, 93.3, 92.5, 85.3, 45.9, 40.0, 39.2, 36.0, 31.9, 26.0, 21.1. MS (FAB$^+$): *m*/Hz 552.0 $[M]^+$, 467.1 $[M - 3CO - H]^+$, 412.1 $[M - Mn(CO)_3 - H]^+$.

Reaction of 5a with 9-Diazofluorene: Formation of 2-[Tricarbonyl{η^6-2′-[tricarbonyl(η^5-fluoren-9-yl)rhenium(I)]phenyl}chromium(0)]-3-methylpyridine (5b) and Tetracarbonyl[2-{η^6-2′-[tricarbonyl(9″-η:fluoren-9″-yl-κC^9)-phenyl}chromium(0)]-3-methylpyridine-κN]rhenium(I) (5c). To a boiling solution of complex **5a** (472 mg, 0.71 mmol) in *n*-heptane/toluene (3:1) (20 mL) was added a solution of 9-diazofluorene (272 mg, 1.42 mmol) in toluene (6 mL) over a total period of 4 h. The reaction mixture was further stirred and boiled for 4 h and cooled to room temperature. The solvents were removed under reduced pressure and the crude mixture dissolved in CH_2Cl_2. Silica gel was added to the resulting solution and the solvent removed under vacuum. The coated silica gel was loaded on the top of a SiO_2 column packed in *n*-hexane at 5 °C. The orange band containing the unreacted starting complex **5a** was recovered with a 1:2 mixture of *n*-hexane and CH_2Cl_2 (66.7 mg). A red band containing a mixture of **5b** and **5c** was eluted with pure CH_2Cl_2. The corresponding solution was stripped of solvents under reduced pressure and submitted to a second chromatography on SiO_2 (15 μm) at 5 °C. Complex **5c** was first eluted with a 1:2 mixture of *n*-hexane and CH_2Cl_2 (109 mg, 20%). Complex **5b** was recovered by elution with pure CH_2Cl_2 (70 mg, 13%). Data for complex **5b** are as follows. High-resolution MS (FAB+): calcd for $C_{31}H_{18}NO_6{}^{52}Cr^{187}Re$ 739.009 687, found 739.010 585. IR (CH_2Cl_2): ν(CO) 2022, 1976, 1928, 1901 cm^{-1}. ^{1}H NMR (C_3D_6O, 500 MHz): δ 8.74 (d, 1H, ^3J = 5.0 Hz), 8.33 (d, 1H, ^3J = 7.8 Hz), 7.99 (d, 1H, ^3J = 8.0 Hz), 7.81 (d, 1H, ^3J = 7.5 Hz), 7.74 (d, 1H, ^3J = 7.7 Hz), 7.62 (t, 1H, ^3J = 6.8 Hz), 7.37 (t, 1H, ^3J = 7.6 Hz), 7.07 (t, 1H, ^3J = 7.2 Hz), 6.98 (t, 1H, ^3J = 7.1 Hz), 6.67 (t, 1H, ^3J = 7.7 Hz), 6.32 (d, 1H, ^3J = 6.6 Hz), 6.29 (d, 1H, ^3J = 6.6 Hz), 6.04 (t, 1H, ^3J = 6.4 Hz), 5.82 (d, 1H, ^3J = 8.3 Hz), 5.69 (t, 1H, ^3J = 6.4 Hz), 3.12 (s, 3H). ^{13}C NMR (C_3D_6O, 125 MHz): δ 234.7 (CO), 198 (CO), 197.5 (CO), 193.0 (CO), 158.5, 152.8, 150.1, 145.7, 145.6, 136.8, 135.0, 134.9, 126.7, 126.6, 125.5, 123.7, 123.1, 123.0, 122.6, 122.5, 120.1, 119.1, 103.2, 102.2, 96.0, 91.0, 90.2, 61.2, 24.0. Data for complex **5c** are as follows. Anal. Calcd for $C_{32}H_{18}NO_7ReCr \cdot {}^2/_3CH_2Cl_2$: C, 47.66; H, 2.37; 1.70. Found: C, 47.53; H, 2.22; N, 1.73. High-resolution MS (FAB+): calcd for $C_{32}H_{18}NO_7{}^{52}Cr^{187}Re$ 767.004 602, found 767.004 281. IR (CH_2Cl_2): ν(CO) 2094 (w), 1997 (s), 1963 (vs), 1936 (s), 1896 (s) cm^{-1}. ^{1}H NMR ($CDCl_3$, 500 MHz): δ 8.87 (d, 1H, ^3J = 5.0 Hz), 8.11 (d, 1H, ^3J = 7.3 Hz), 7.94 (d, 1H, ^3J = 7.7 Hz), 7.87 (m, 2H), 7.43 (t, 1H, ^3J = 7.5 Hz), 7.30 (m, 1H), 7.20 (t, 1H, ^3J = 7.3 Hz), 7.10 (t, 1H, ^3J = 7.2 Hz), 6.82 (t, 1H, ^3J = 7.7 Hz), 6.20 (d, 1H, ^3J = 5.7 Hz), 5.86 (d, 1H, ^3J = 8.0 Hz), 5.69 (t, 2H, ^3J = 6.0 Hz), 5.32 (t, 1H, ^3J = 6.4 Hz), 3.10 (s, 3H). ^{13}C NMR ($CDCl_3$, 125 MHz): δ 232.5 (CO), 189.6 (CO), 187.9 (CO), 187.3 (CO), 187.1 (CO), 159.2, 156.4, 153.9, 152.6, 145.1, 135.7, 134.5, 134.4, 125.9, 125.8, 125.7, 125.5, 123.9, 123.6, 123.0, 120.6, 120.5, 119.5, 100.8, 99.6, 93.5, 88.9, 87.7, 50.6, 24.8.

Synthesis of 2-[Tricarbonyl(η^5-fluoren-9-yl)manganese]-acetophenone (6b). Conditions and reagents for this reaction are as follows: complex **6a** (344 mg, 1.20 mmol), *n*-hexane/toluene (1:1, 15 mL), ebullition; 9-diazofluorene (461 mg, 2.40 mmol), toluene (5 mL), dropwise addition for 45 min. Flash chromatography with a SiO_2 column packed in *n*-hexane at 5 °C: **6b** (3:2 CH_2Cl_2/acetone), yellow light cotton-like solid (0.41 g, 0.98 mmol, 82% yield). Anal. Calcd for $C_{24}H_{15}O_4Mn$: C, 68.26; H, 3.58. Found: C, 67.51; H, 3.75. High-resolution MS (EI): calcd for $C_{24}H_{15}O_4Mn$ *m*/Hz 422.0351, found 422.0350. IR (CH_2Cl_2): ν(CO) 2017 (s), 1934 (vs); ν(C=O) 1721 (w). ^{1}H NMR ($CDCl_3$, 500 MHz): δ 8.30 (d, 1H, ^3J = 7.5 Hz), 8.15 (m, 2H), 7.79 (t, 1H, ^3J = 7.5 Hz), 7.73 (d, 1H, ^3J = 7.7 Hz), 7.59 (t, 1H, ^3J = 7.7 Hz), 7.29 (m, 6H), 1.84 (s, 3H). ^{13}C NMR ($CDCl_3$, 125 MHz): δ 224.9 (CO), 201.9, 142.4, 136.9, 132.1, 130.5, 128.8, 128.7, 128.4 (2C), 125.3 (2C), 125.0 (2C), 123.2 (2C), 107.9, 93.1, 84.1, 29.2. MS (EI): *m*/Hz 422 $[M]^+$, 394 $[M - CO]^+$, 366 $[M - 2CO]^+$, 338 $[M - 3CO]^+$, 333 $[M - 3CO - Mn]^+$, 289 $[M - 3CO - Mn - HC(O)CH_3]^+$.

Acknowledgment. We gratefully acknowledge the support provided by the Centre National de la Recherche Scientifique and the Deutsche Forschungsgemeinschaft. Z.R. particularly thanks the CNRS for the financial support provided through an associate-researcher fellowship. We also thank Maxime Bernard and Professor Jean-Jacques André from the Institute Charles Sadron for their contribution in the acquisition and analysis of the ESR data.

Supporting Information Available: Listings of crystallographic and structural data for compounds **1b**,**c**, **2b**, **3c**−**e**, and **5a**,**c**; these data are also available as CIF files. This material is available free of charge via the Internet at http://pubs.acs.org.

OM020116Z